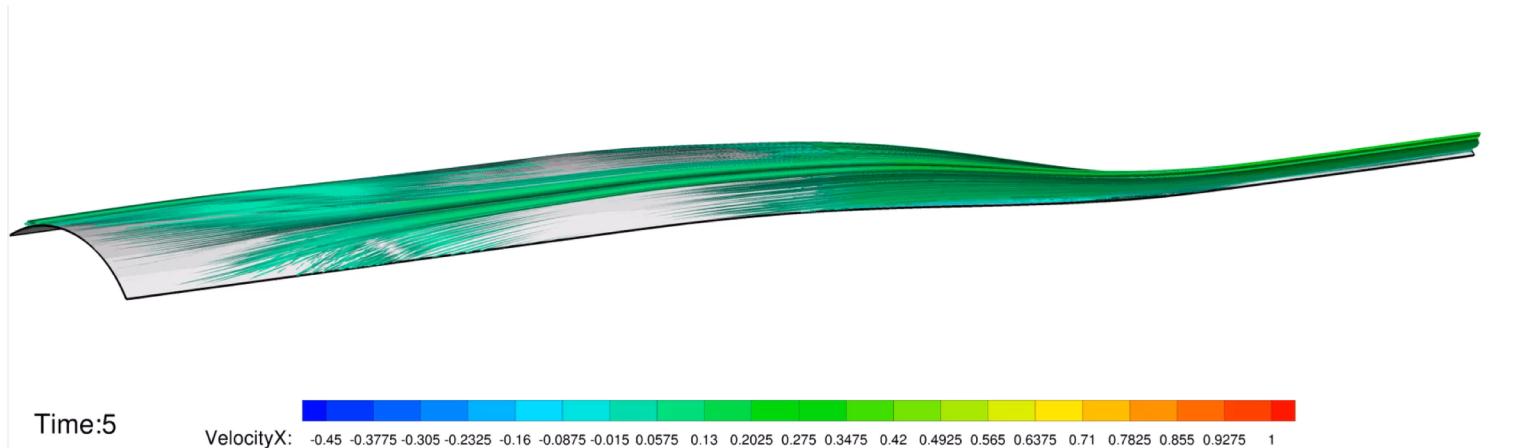


A fast pressure-correction method for incompressible flows over curved walls



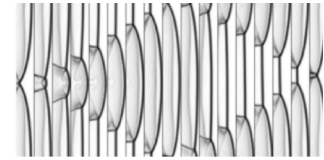
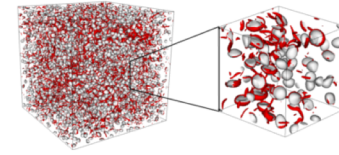
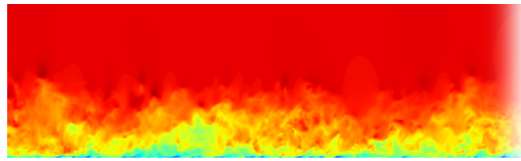
Antonino Ferrante

Aeronautics & Astronautics
University of Washington, Seattle

PhD research of Abhiram Aithal



Advanced Modeling & Simulation Seminar Series
NASA Ames Research Center, February 21, 2019



Outline

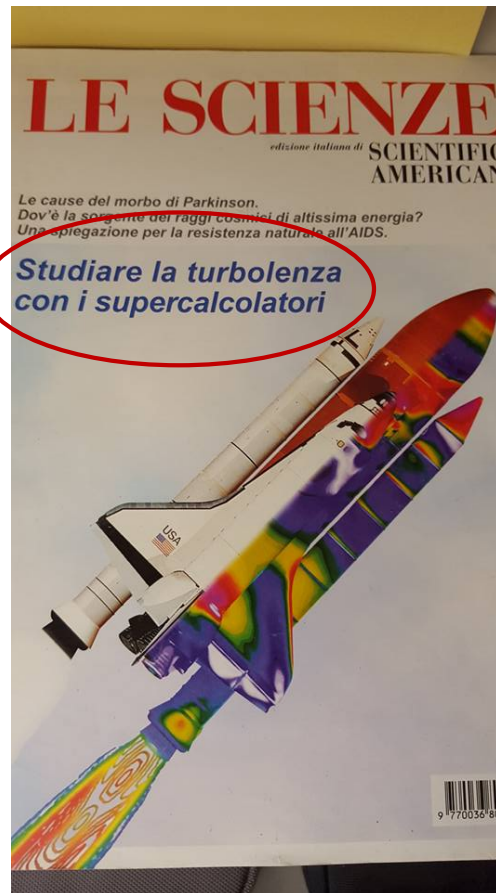
- What motivates me to be involved in turbulence research?
- Computational Fluid Mechanics (CFM) group at the UW
- A fast pressure correction method to solve incompressible flows over curved walls
 - Motivation
 - Background
 - Numerical method
 - Orthogonal formulation of NS eqs
 - FastPoc: fast Poisson solver in orthogonal coordinates
 - FastRK3: fast NS solver w RK3
 - Results
 - Verification & Validation
 - Applications

What motivated me to pursue turbulence research in the 90's?

1990's B.S. in
Aeronautical
Engineering at the
Universita' di
Napoli, Federico II

1996-97 M.S. from
von Karman
Institute for fluid
dynamics

1997 back in
Italy and read
Le Scienze



JOURNAL ARTICLE **Tackling Turbulence with Supercomputers**

Parviz Moin and John Kim

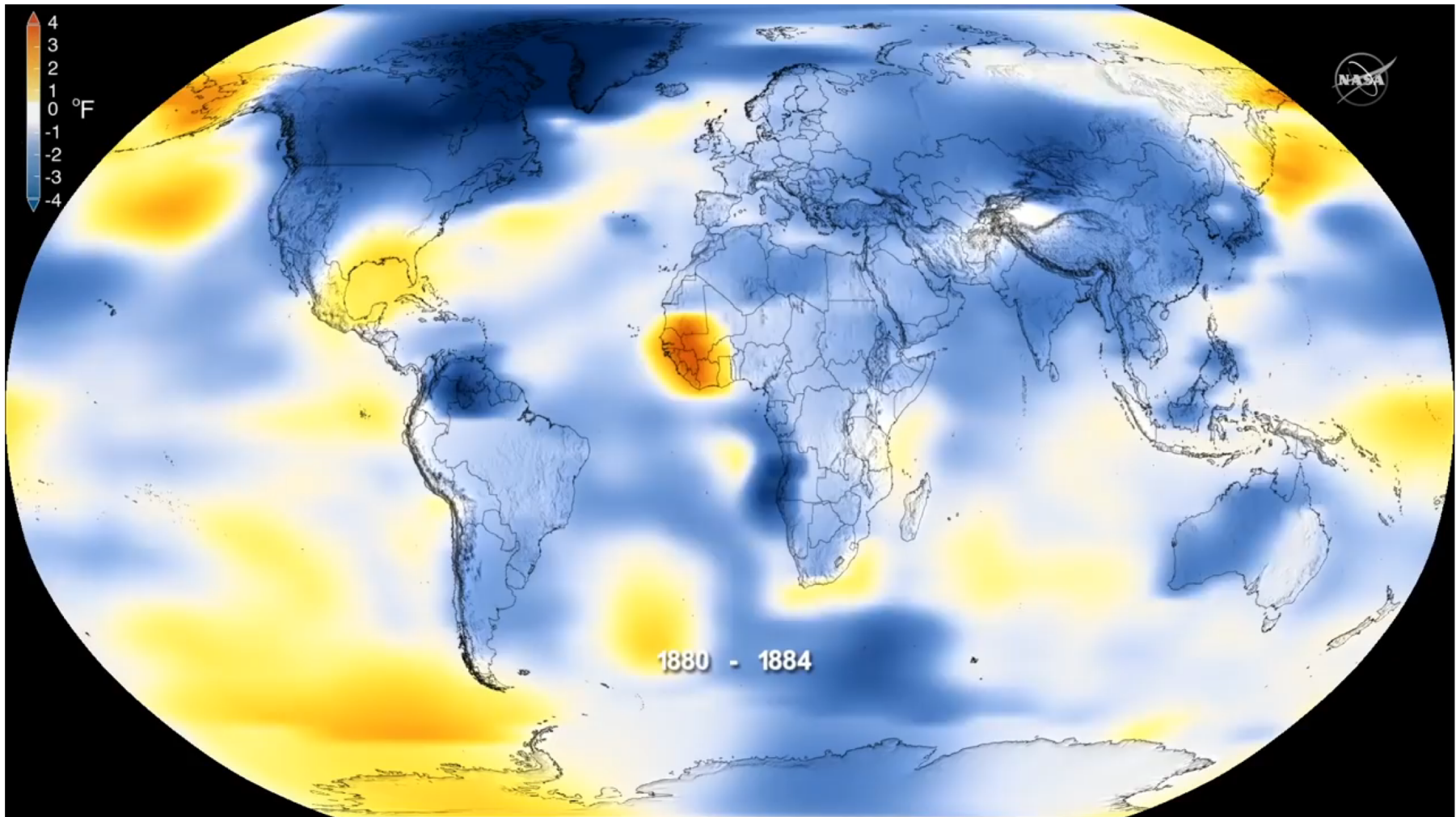
Scientific American

Vol. 276, No. 1 (JANUARY 1997), pp. 62-68

You can say it's
Parviz' fault!

Since the 1880s, the average global surface Earth temperature has risen about 2° F (~1° C).

What motivates me today to continue turbulence research?
2018 fourth warmest year in continued warming trend (NASA & NOAA)



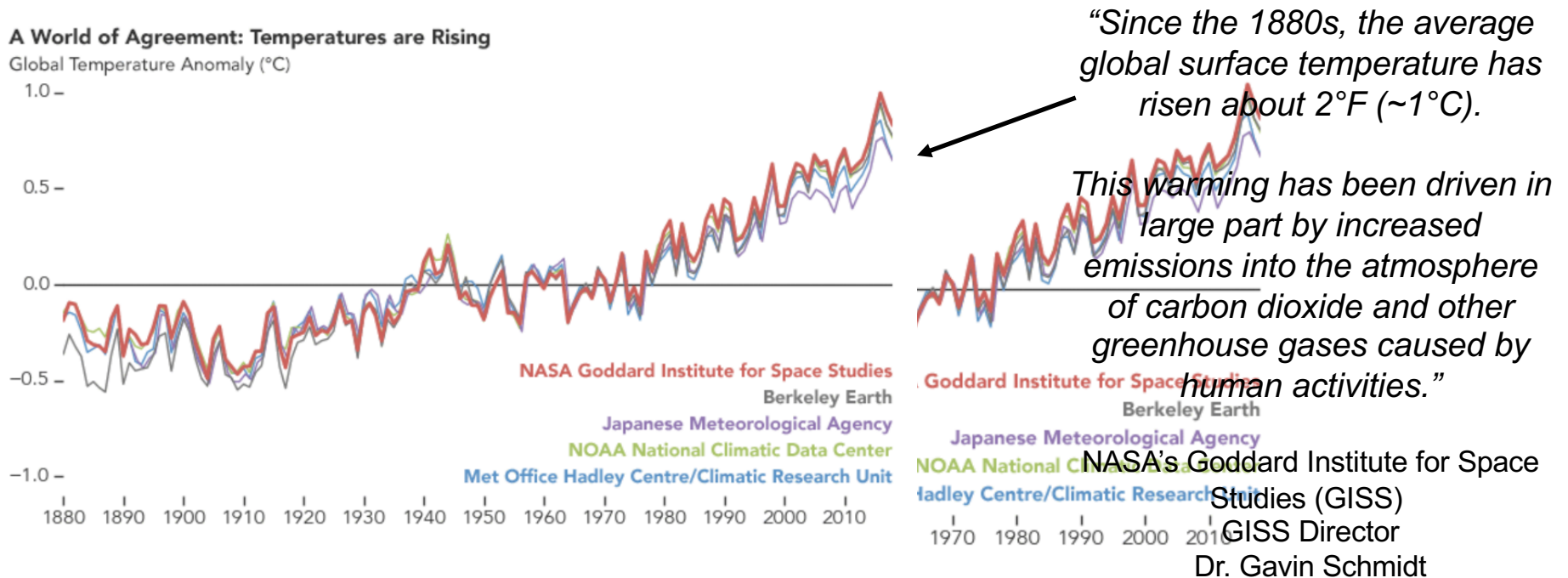
<https://svs.gsfc.nasa.gov/13142>

<https://climate.nasa.gov/news/2841/2018-fourth-warmest-year-in-continued-warming-trend-according-to-nasa-noaa/>

What inspires me today to continue turbulence research? Climate Change

The 5th Assessment Report of the Intergovernmental Panel on Climate Change 2013:

"Warming of the climate system is unequivocal."



Global temperatures in 2018 were 1.5°F (0.83 °C) higher than the mean between 1951 to 1980 (NASA)

<https://svs.gsfc.nasa.gov/13142>
<https://climate.nasa.gov/news/2841/2018-fourth-warmest-year-in-continued-warming-trend-according-to-nasa-noaa/>

Effects of and Reasons for Global Warming

Effects

- GISS Director Dr. Gavin Schmidt:
“The impacts of long-term global warming are already being felt — in coastal flooding, heat waves, intense precipitation and ecosystem change.”
- Biologists say: one in five species on Earth now faces extinction, and that will rise to 50% by the end of the century unless urgent action is taken. (The Guardian)

Reasons

- IPCC 2013: *“Total radiative forcing is positive, and has led to an uptake of energy by the climate system. The largest contribution to total radiative forcing is caused by the increase in the atmospheric concentration of CO₂ since 1750”.*
- IPCC 2009: *“The combustion processes in electric power plants, jet engines, gasoline and diesel powered vehicles are the primary sources of carbon dioxide (CO₂) emissions. Global increases in concentrations of CO₂ are mainly due to this fossil fuel use. CO₂ annual emissions grew by about 80% between 1970 and 2004.”*

Living in Balance

- *“Sit, be still, and listen, because you’re drunk and we’re at the edge of the roof” ~ Rumi*
- *“When the animals come to us asking for our help, will we know what they are saying? When the plants speak to us in their delicate, beautiful language, will we be able to answer them? When the planet herself sings to us in our dreams, will we be able to wake ourselves and act?” ~ Gary Loles*
- We need to *‘wake up’* to learn to live in balance with all living organisms and the ecosystems of the Earth cause we are not separate selves from the rest of the Universe and, at this point, as humans we don’t really have a choice for survival. And even if we were too late, at least, we tried...

- *“What is the Earth asking from me?” ~ Tara Brach**

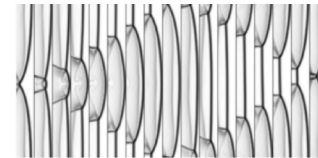
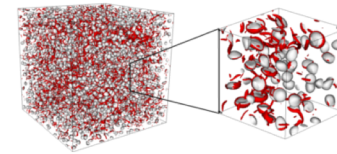
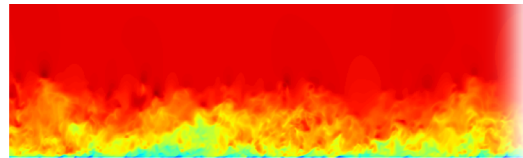
- What is Life asking from me?



* <https://www.tarabrach.com/earths-crisis/>

The Science part...

- Unfortunately, in the foreseeable future, our dependency on fossil fuels is not suddenly going to change.
- In order to help stabilize, and hopefully reverse, anthropogenic CO₂ emissions we should reduce fossil fuel consumption by improving combustion efficiency and by reducing the drag of vehicles, and invest in renewable energy and alternative transport as well.
- To do so,
 - We must better understand the *physics of wall-turbulence*
(Aerodynamics)
 - We must better understand the *physical and chemical processes involved in the atomization, evaporation and combustion of liquid fuels*
(Propulsion)



Computational Fluid Mechanics (CFM)

Graduated Ph.D.



Lt. Col. Barrett
McCann, Ph.D. 2014
Faculty at USAF
Academy, Colorado



Michael Dodd
Ph.D. 2017
Postdoc at CTR
Stanford University

Ph.D. students



Abhiram Aithal



Pablo Trefftz-Posada



Andreas Freund



Madeline Samuelli

The CFM group conducts fundamental research in fluid mechanics.

The main research focus of the group is to explain the *physical mechanisms* of **single-phase, multi-phase, and multi-species turbulent flows** for **aerodynamics**, and **propulsion**.

The CFM group develops models, numerical methods and parallel algorithms for **DNS and LES of turbulent flows** using high-performance computing (HPC) to unravel the physical mechanisms of turbulent flows.

Graduated M.S.

- Dawei Lu (M.S. In Progress)
- Alex Lee (M.S., 2016)
- Christopher Uyeda (M.S., 2015)
- Irfan Syahdan (M.S., 2015)
- Sean McMahon (M.S., 2014)
- Zhengcheng Gu (M.S., 2014)
- Keegan Webster (M.S., 2013)
- Hezky Varon (M.S., 2012)

Undergraduate students

- 13 UG students involved in research since 2009
- 8 URM students (2 Ph.D., 2 M.S., 4 UGs)

Motivation for DNS of wall-bounded turbulence

Aerodynamics

Aft-body flow



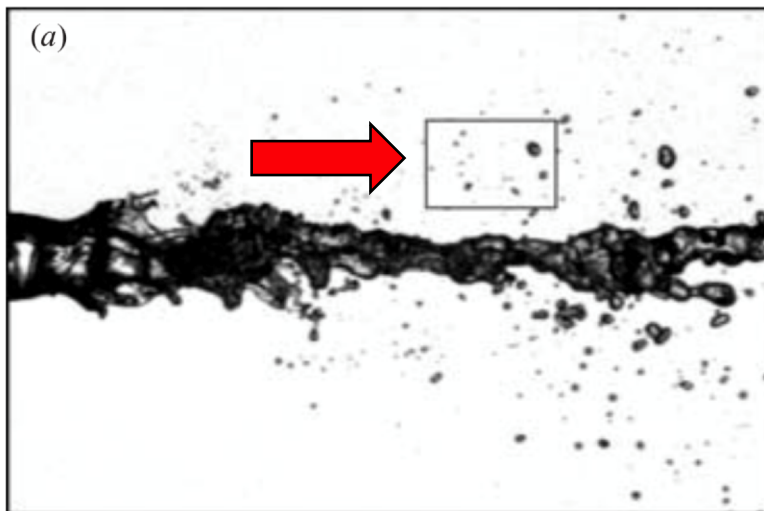
- Design of aft-bodies currently rely upon turbulence wall-models
- RANS wall-models fail in this situation of incipient flow separation or for separated flows, e.g., high angles of attack at take-off and landing
- NASA's CFD Vision 2030:
 - Improve CFD modeling of turbulent flow separation
- DNS does not make use of empirical assumptions and can be used to improve RANS models

Motivation for DNS of multiphase turbulence

Propulsion

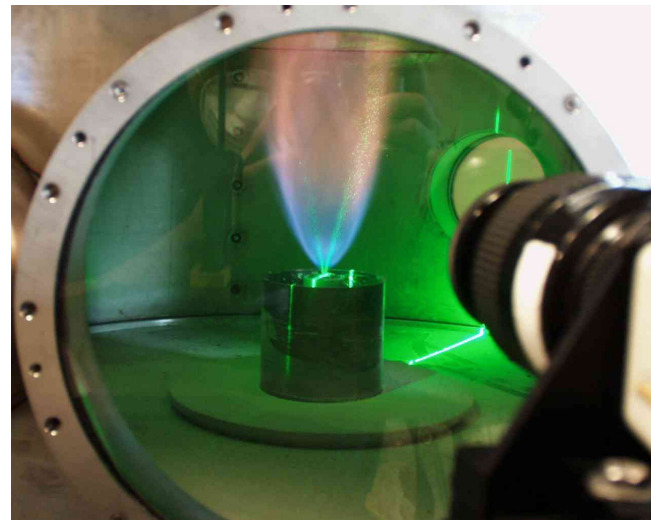
- Droplet-laden turbulent flows occur in gas-turbine engines
 - Spray atomization and droplet combustion
 - Physical mechanisms of finite-size droplets and turbulence interaction are largely unknown
 - LES and RANS models need physical understanding and data to be tuned

Spray Atomization



Marmottant et al. (2004)

Spray Combustion



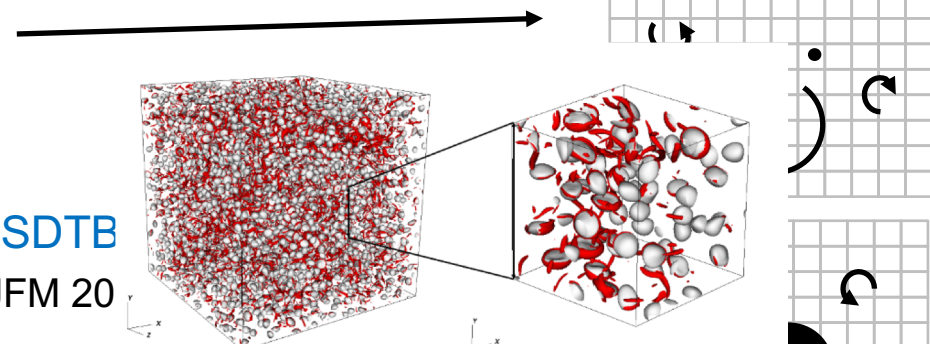
NIST spray combustion test bed

A humble start...

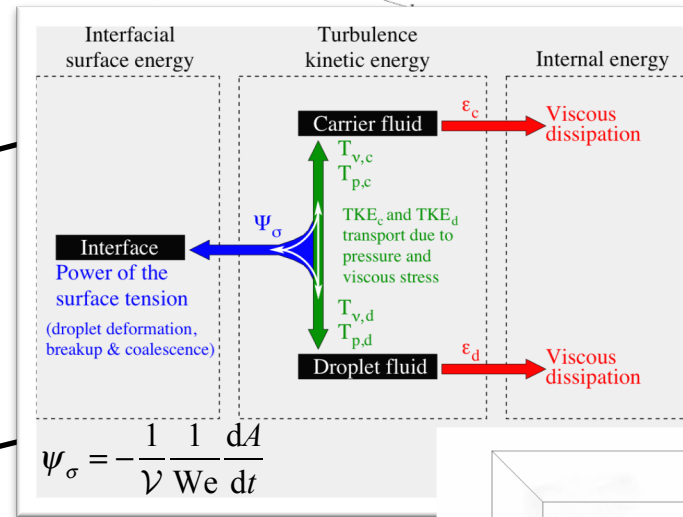
Contributions to Multiphase Turbulence

"a few highlights"

- **$D < \eta$ point-particle approach**
 - Two-way coupling particle-laden HIT
 - Ferrante & Elghobashi (PoF 2003)
 - Drag reduction with microbubbles in SDTB
 - Ferrante & Elghobashi (JCP 2004, JFM 20)
 - Particle dispersion in SDTBL
 - Dodd & Ferrante (ICMF 2013)

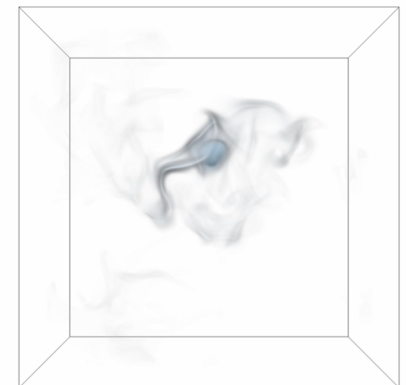


- **$D > \eta$ finite-size solid particles**
 - Two-way coupling particle-laden HIT
 - Lucci & al. (JFM 2010, PoF 2011)



- **$D > \eta$ finite-size deformable droplets**
 - Droplet-laden HIT
 - Baraldi & al. (CaF 2014), Dodd & Ferrante (JCP 2014, JFM 2016)
 - Evaporating droplet-laden homogeneous turbulence
 - Dodd & Ferrante (APS-DFD, ICMF)

$$\psi_\sigma = -\frac{1}{\nu} \frac{1}{We} \frac{dA}{dt}$$



A Wall Model for Large-Eddy Simulation of Compressible Channel Flows

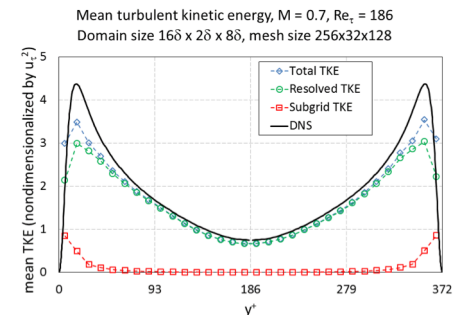
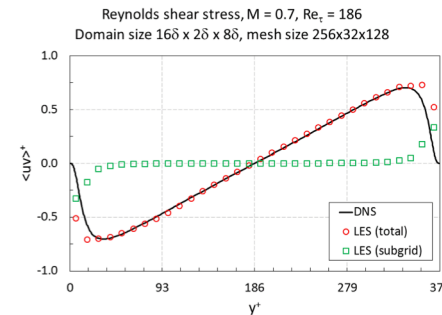
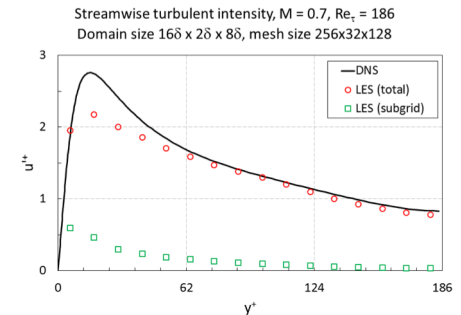
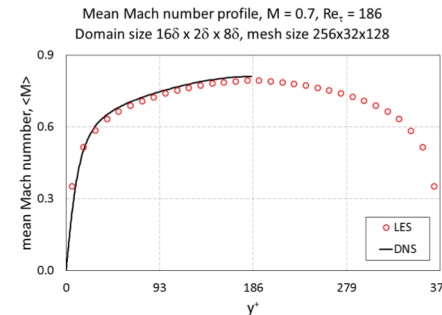
Barrett T. McCann

Head, Dept of Aeronautics, US Air Force Academy, Colorado

Ph.D. 2014

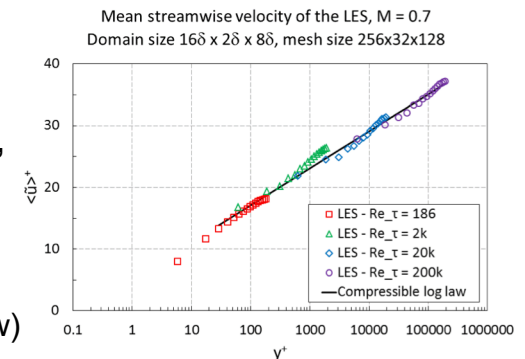


- Objective: develop a new parameter-free wall model for LES of compressible high-Re channel flows
 - Avoid wall-resolved LES grid size requirement of $O(Re^{13/7})$
- Approach: extend to compressible flows the wall model for incompressible channel flows by Chung and Pullin (*J. Fluid Mech.* 2009)
- Wall model avoids resolving steep near-wall velocity & temperature gradients by integrating the LES momentum, internal energy equations from wall to first grid point
- 2 resulting ODEs provide local, instantaneous wall shear-stress and heat-flux BCs
- Results compare well to incompressible DNS of Hoyas and Jiménez (*Phys. Fluids* 2006), $M = 0.7$ DNS of Wei and Pollard (*Comp. & Fluids* 2011)
 - $16\delta \times 2\delta \times 8\delta$ computational domain,
 - $256 \times 32 \times 128$ grid points



LES compared to DNS of Wei and Pollard (CaF 2011)

Predictions for $M = 0.7$,
 $Re_\tau = 186, 2 \times 10^3,$
 $2 \times 10^4, 2 \times 10^5$



McCann & Ferrante (Under Review)

DNS of droplet-laden isotropic turbulence

Michael S. Dodd

Postdoctoral Fellow, Center for Turbulence Research, Stanford University
Ph.D. 2017



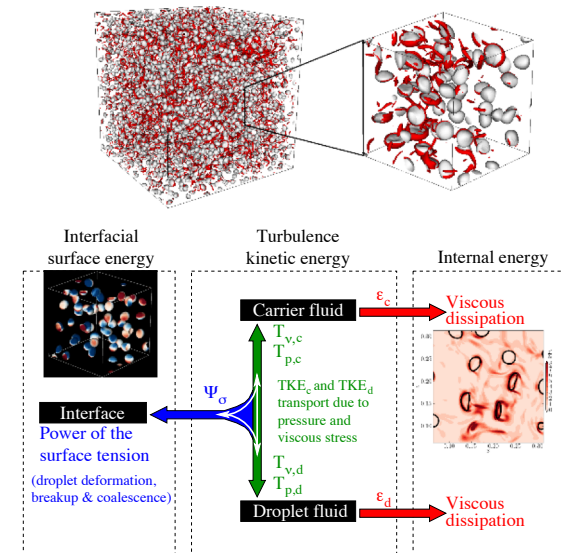
- Motivation
 - Spray combustion & cloud physics
 - Physical mechanisms of droplet/turbulence interaction
 - Droplet vaporization in turbulence
- Numerical method
 - Mass conserving, consistent, wisps-free **volume-of-fluid** method (**CaF 2014 [1]**)
 - Pressure-correction method based on FFT-based Poisson solver for pressure, **FastP*** (**JCP 2014 [2]**)
 - Coupled NS/VoF solver 10-40 time faster than multigrid-based methods
 - Verified for density and viscosity ratios up to 10,000
 - Validated for falling water droplet in air and vaporizing/condensing droplets

[1] Baraldi, A., Dodd, M. S. & Ferrante, A. "A mass-conserving volume-of-fluid method: volume tracking and droplet surface-tension in incompressible isotropic turbulence." *Computers and Fluids*, **96**, 322-337, 2014

[2] Dodd, M. S. & Ferrante, A. "A fast second-order pressure-correction method for two-fluid flows." *Journal of Computational Physics*, **273**, 416-434, 2014

[3] Dodd, M. S. & Ferrante, A. "On the interaction of Taylor length scale size droplets and isotropic turbulence." *Journal of Fluid Mechanics*, **806**, 356-412, 2016

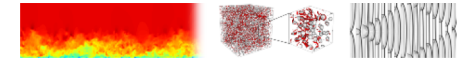
Physical mechanisms of droplet-turbulence interaction (*JFM* 2016 [3])



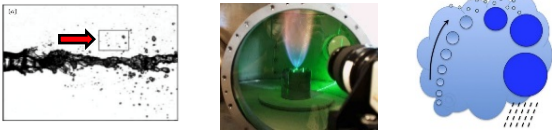
Droplet vaporization in isotropic turbulence



- Vaporization rate from the DNS is in excellent agreement with the experimental data by Birouk & Fabbro *PCI* (2013)



Motivation



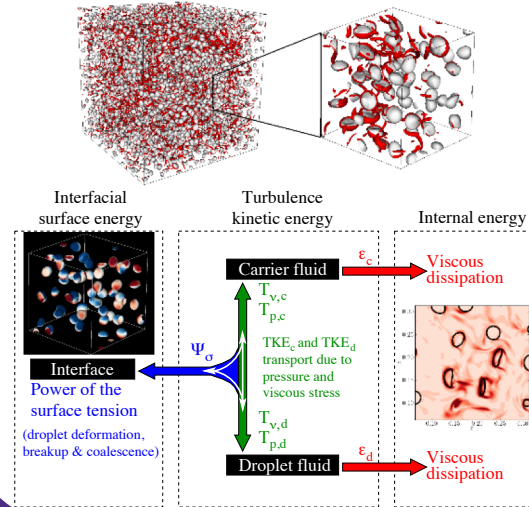
- Spray combustion & cloud physics
- Physical mechanisms of droplet/turbulence interaction
- Droplet vaporization in turbulence

Numerical methods of MultiFlow: FastP* with VoF

- Mass conserving, consistent, wisps-free **volume-of-fluid** method (*CaF* 2014)
- Pressure-correction method based on FFT-based Poisson solver for pressure, **FastP*** (*JCP* 2014)
- Coupled NS/VoF solver 10-40 time faster than multigrid-based methods
- 2nd-order accurate in space and time for velocity
- Verified for density and viscosity ratios up to 10,000
- Validated for falling water droplet in air and vaporizing/condensing droplets

Verified/Validated/Scalable

Flow physics of droplet-laden isotropic turbulence (*JFM* 2016)



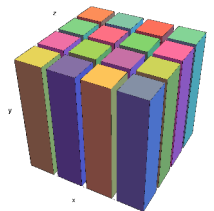
Droplet vaporization in isotropic turbulence



- Vaporization rate from the DNS is in excellent agreement with the experimental data by Birouk & Fabbro *PCI* (2013) at $Re_\lambda = 25$

PSH3D: fast Poisson solver for petascale DNS

- Parallel 2D FFT
- Parallel Linear Solver in the third direction
- Scalable up to 262k cores of Blue Waters
- Solves the Poisson equation in 1 sec for 8192^3 grid points using 131k cores



2D Domain
Decomposition

References

- Dodd & Ferrante *JFM* (2016)
- Adams, Dodd, Ferrante *ICTAM* (2016)
- Dodd & Ferrante *JCP* (2014)
- Baraldi, Dodd & Ferrante *CaF* (2014)

Acknowledgments

- Michael Dodd, Ph.D. student
- Darren Adams, NCSA
- NSF CAREER Award
- UW E-Science / Hyak

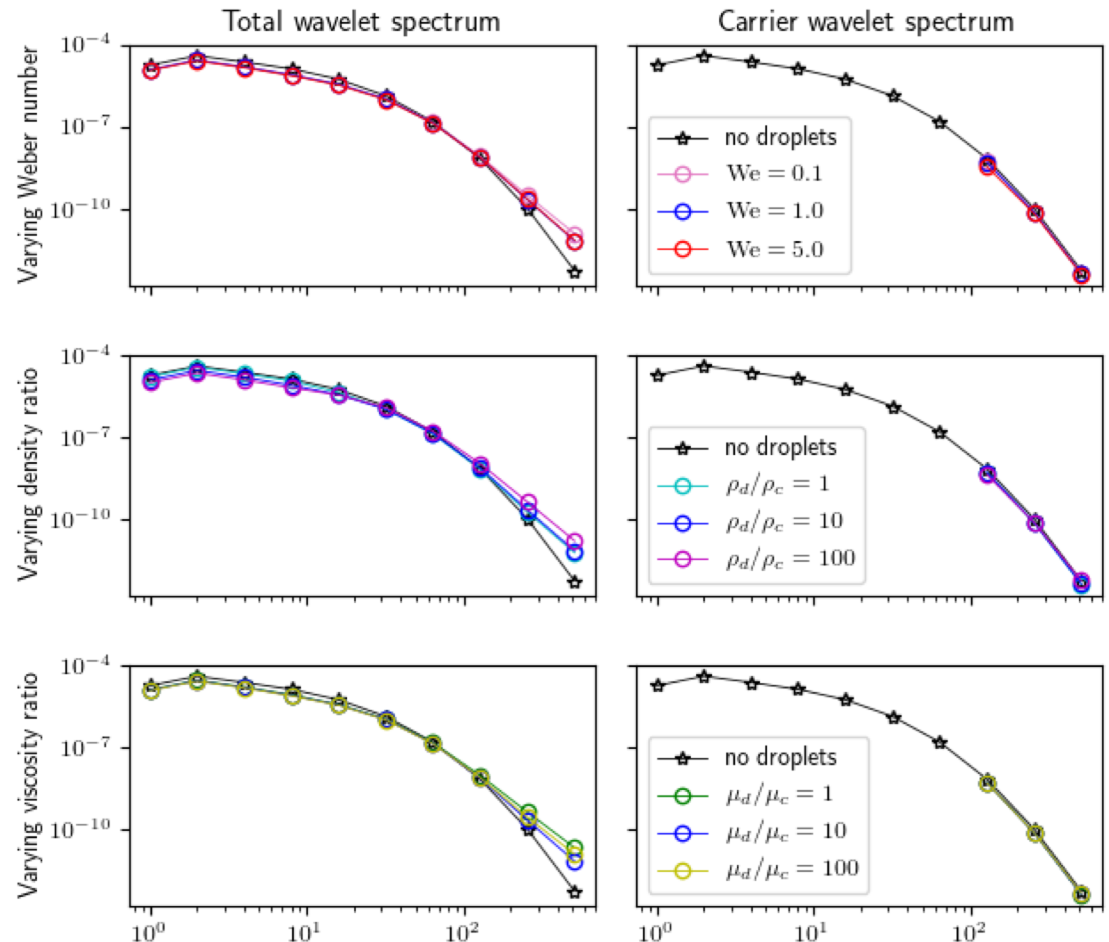


Wavelet-spectrum analysis of droplet-laden isotropic turbulence



Andreas Freund

- The energy spectrum of isotropic turbulence laden with droplets of Taylor-length-scale size shows an increase and oscillations at high wavenumbers.
- These effects are due to the Fourier transform's difficulty in capturing the sharp velocity gradients at the interface.
- An alternative definition of the energy spectrum uses the wavelet transform.
- The wavelet transform preserves spatial information, so effects of sharp gradients remain localized.
- We are also able to decompose our spectra into carrier, droplet, and interfacial parts.
- The wavelet spectra give us three main results:
 - The carrier energy at high wavenumbers remains unaffected by the droplets.
 - The droplets cause an increase in energy near the interface due to the effects of the sharp velocity gradients (as with the Fourier spectrum).
 - The denser droplets decrease energy at low wavenumbers due to an increase in dissipation.

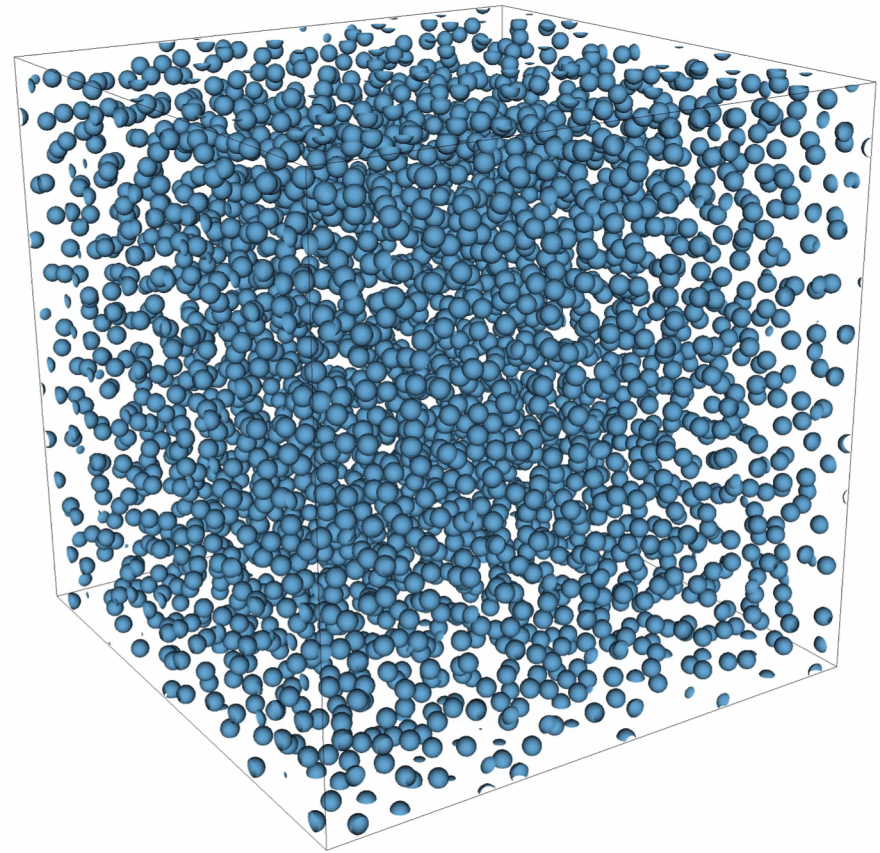


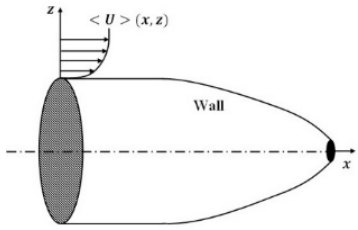
DNS of droplet-laden homogeneous shear turbulence



Pablo Trefftz Posada

- We have developed a flow solver to conduct DNS of droplet-laden homogeneous shear turbulence.
- Shear acts as a source in the TKE budget, and we want to analyze the pathways of TKE with this added source.
- We have found that compared to single-phase flow, Taylor-length scale size droplets in homogeneous shear turbulence:
 - Reduce TKE by $\sim 10\%$ - 20%
 - Enhance dissipation of TKE
 - Reduce production of TKE
- We are studying how the increased droplet deformation due to shear affects the power of the surface tension and the TKE budget dynamics.

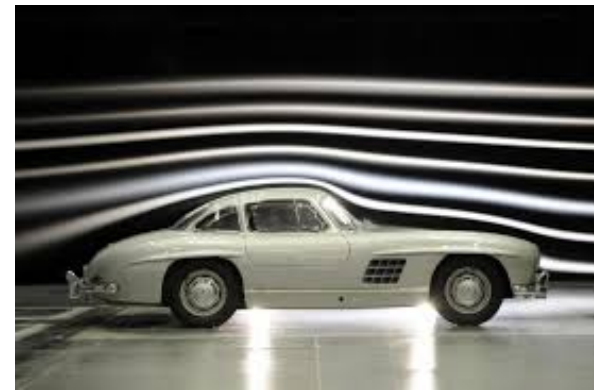




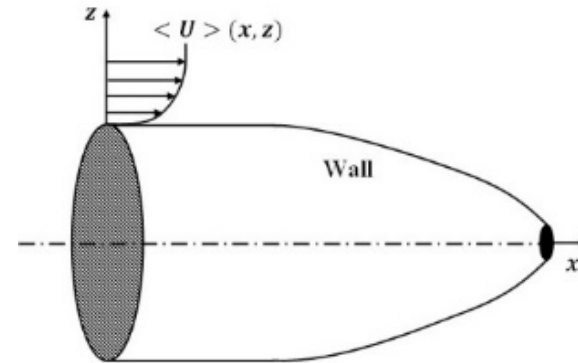
A fast pressure-correction method for incompressible flows over curved walls



Abhiram Aithal



Motivation



- Design of curved bodies (eg. aft-bodies) currently relies upon **RANS turbulence wall-models**
- **RANS wall-models** *fail* in predicting **incipient and full separation**

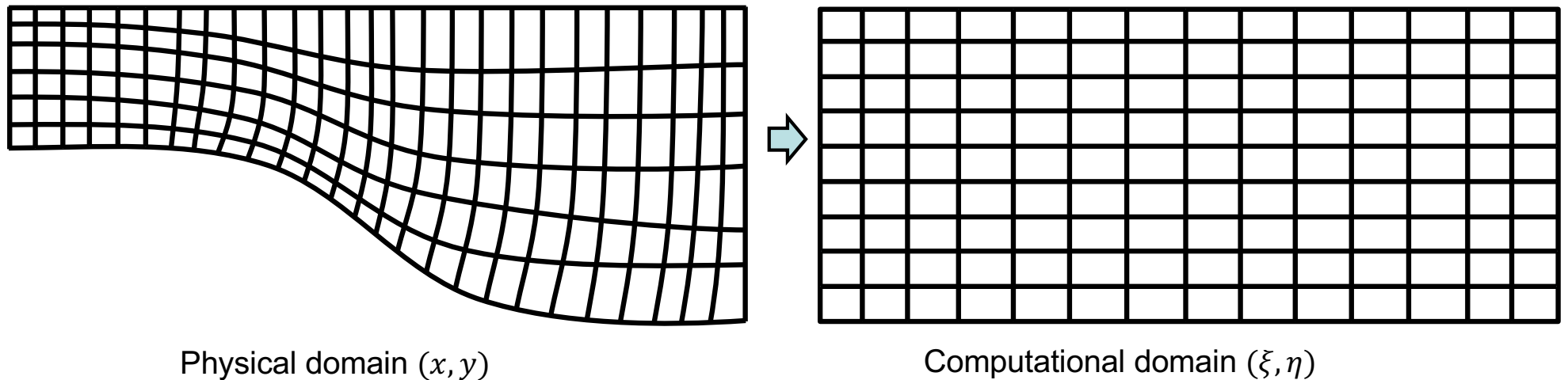
NASA CR 2014 - CFD Vision 2030: A Path to Revol. Comput. Aerosc.

- **DNS** does not make use of empirical assumptions \Rightarrow
 \Rightarrow the results can *explain the physics and provide statistics* which help to *develop and improve* **RANS and LES wall-models**
- The proposed *fast pressure-correction method* can be used to solve the NS equations over curved surfaces also with LES and RANS

Objectives

- Develop a pressure-correction method to perform DNS of turbulent flows over curved surfaces which is
 - Sufficiently Accurate
 - 2nd - 3rd order accuracy in space and time
 - Efficient
 - Explicit time-integration scheme
 - FFT-based Poisson solver for pressure which is $O(10-100)$ times faster than iterative solvers like multigrid
 - Scalable
 - Scales well on thousands of computing cores
 - Extendable to Petascale

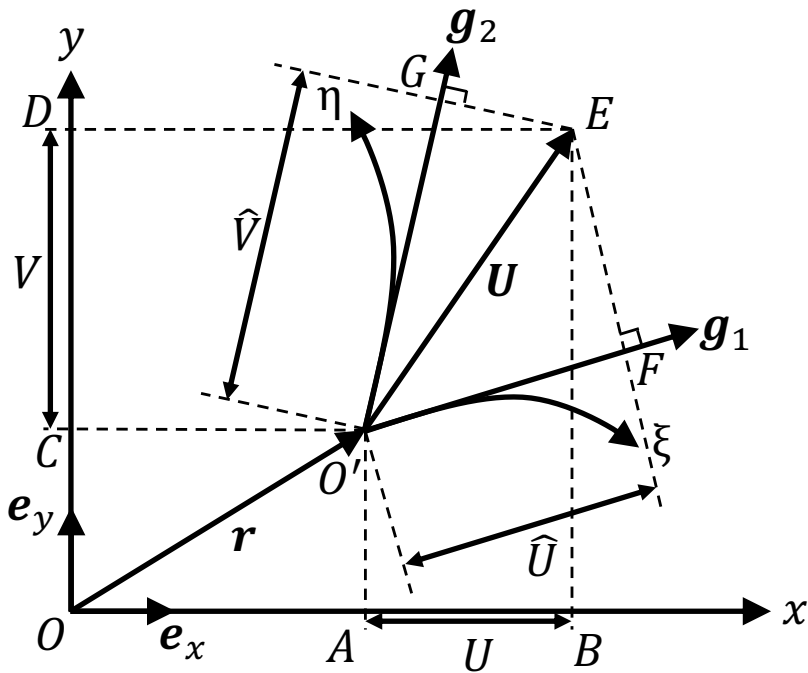
Background: NS eqs in curvilinear coordinates



- DNS requires discretizing the Navier-Stokes (NS) eqs. on a curved mesh
- NS equations in *general* curvilinear coordinates have been solved via:
 1. Finite volume method (Rosenfeld et al., *JCP* 1991)
 2. Partial transformation of the incompressible NS eqs (Choi et al., *JFM* 1993)
 3. Complete transformation of the incompr. NS eqs (Ge & Sotiropoulos, *JCP* 2007)
 4. Finite/spectral-element method (e.g., NEK5000)
 5. **Orthogonal formulation for vorticity (Nikitin, *JCP* 2006.[†])**

[†] Nikitin, *JCP* 2006 considered only standard orthogonal coordinates: cylindrical, spherical, etc.

Incompressible NS eqs in *general* curvilinear coordinates



In Cartesian coordinates, $\mathbf{U} = \overline{AB} + \overline{CD} = U\mathbf{e}_x + V\mathbf{e}_y$ where \mathbf{e}_x and \mathbf{e}_y are Cartesian basis vectors; in curvilinear coordinates, $\mathbf{U} = \overline{O'F} + \overline{O'G} = \hat{U}\mathbf{g}_1 + \hat{V}\mathbf{g}_2$ where \mathbf{g}_1 and \mathbf{g}_2 are covariant basis vectors

- $\hat{U}^i = (\hat{U}, \hat{V}, \hat{W})$ are the contravariant components of velocity vector

- Metric tensor, g_{ij} (9 terms):

$$g_{ij} = \sum_{k=1}^3 \frac{\partial x^k}{\partial \xi^i} \frac{\partial x^k}{\partial \xi^j}$$

- Christoffel symbol of second kind, Γ_{jk}^i (27 terms):

$$\Gamma_{jk}^i = \frac{1}{2} g^{ip} \left[\frac{\partial g_{pj}}{\partial \xi^k} + \frac{\partial g_{pk}}{\partial \xi^j} - \frac{\partial g_{jk}}{\partial \xi^p} \right]$$

- Covariant derivative operator, ∇_k :

$$\nabla_k \hat{U}^j = \frac{\partial \hat{U}^j}{\partial \xi^k} + \Gamma_{ik}^j \hat{U}^i$$

- Navier-Stokes equations for an incompressible fluid in curvilinear coordinates are:

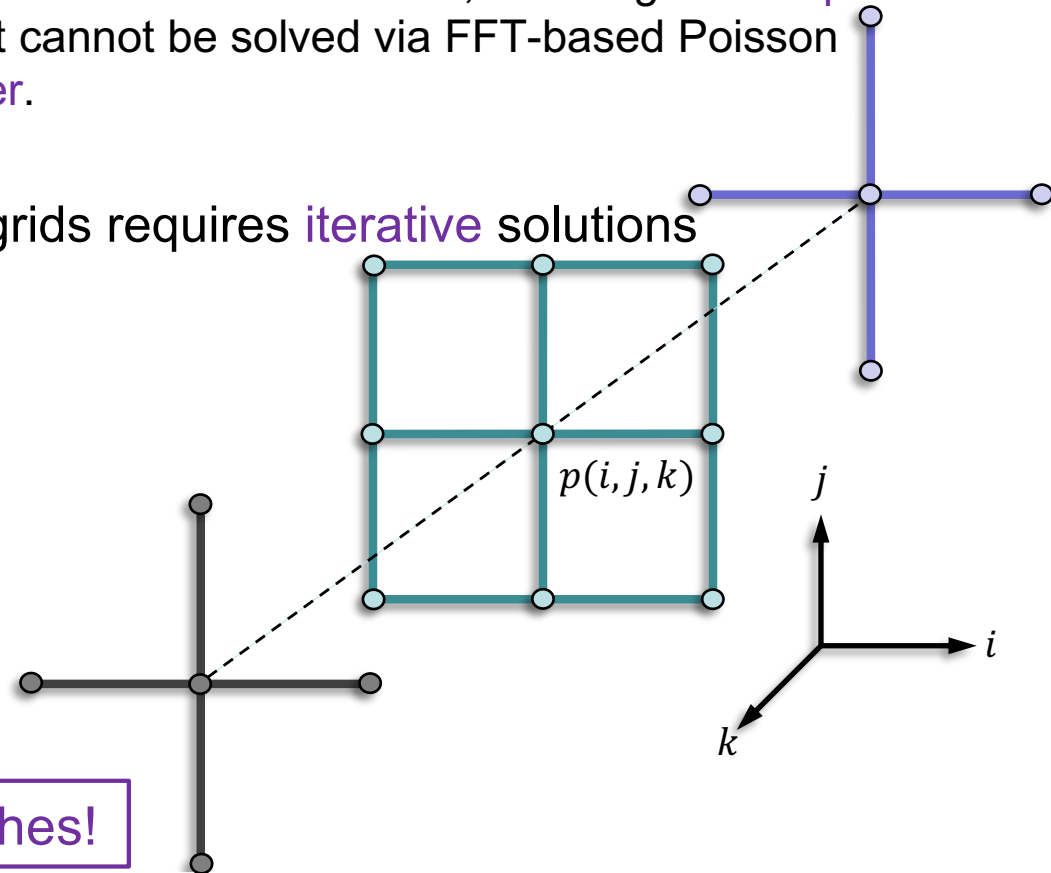
$$\nabla_i \hat{U}^i = 0$$

$$\frac{\partial \hat{U}^i}{\partial t} + \nabla_j \hat{U}^i \hat{U}^j = -\frac{1}{\rho} g^{ij} \nabla_j p + \nu g^{jk} \nabla_{jk}^2 \hat{U}^i$$

Disadvantages of solving Navier-Stokes equations in *general (non-orthogonal)* curvilinear coordinates

- 2. & 3. PT & CT of NS Eqs.
 - 18 unique components of the Christoffel symbol of the second kind Γ_{kj}^i , and 6 unique components of the metric tensor g_{ij} are expensive to compute and store
- 1. FVM, 2. & 3. PT & CT of NS Eqs.
 - Discrete Poisson equation for pressure has cross derivatives, resulting in a 19-point stencil (2nd order central-difference): it cannot be solved via FFT-based Poisson solver, thus requires an iterative solver.
- 4. FEM/SEM: usage of unstructured grids requires iterative solutions

$$g = \begin{array}{|c|c|c|} \hline g_{11} & g_{12} & g_{13} \\ \hline g_{12} & g_{22} & g_{23} \\ \hline g_{13} & g_{23} & g_{33} \\ \hline \end{array}$$

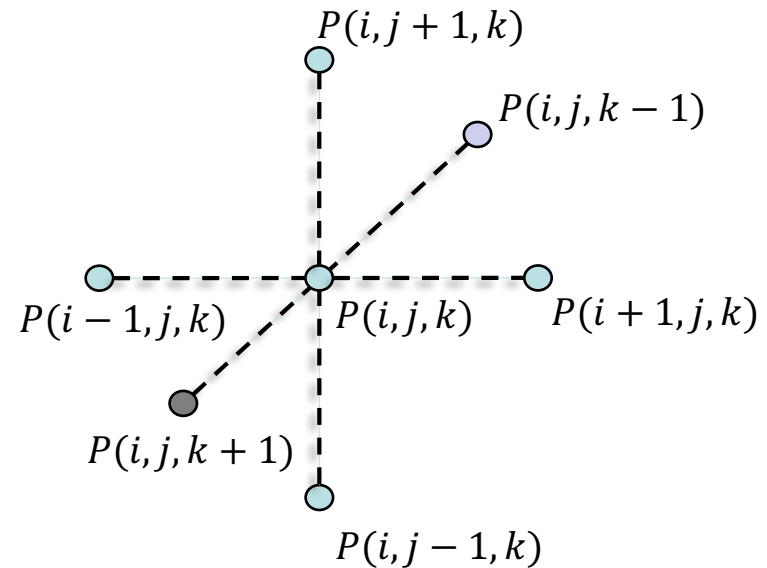


Thus, we do NOT pursue these approaches!

Incompressible Navier-Stokes equations in *orthogonal* curvilinear coordinates

- NS equations are **greatly simplified** in *orthogonal curvilinear coordinates* because $g_{ij} = 0 \forall i \neq j$
- Compute **only the 3 non-zero diagonal terms** of the metric tensor
- Zero off-diagonal terms in the metric tensor \Rightarrow **no cross-derivatives** in NS \Rightarrow Discrete Poisson equation for pressure has **7-point stencil** as in the Cartesian formulation \Rightarrow **FFT-based Poisson** solver can be formulated

$$\mathbf{g} = \begin{array}{|c|c|c|} \hline g_{11} & 0 & 0 \\ \hline 0 & g_{22} & 0 \\ \hline 0 & 0 & g_{33} \\ \hline \end{array} = \begin{array}{|c|c|c|} \hline h_{\xi}^2 & 0 & 0 \\ \hline 0 & h_{\eta}^2 & 0 \\ \hline 0 & 0 & h_{\zeta}^2 \\ \hline \end{array}$$



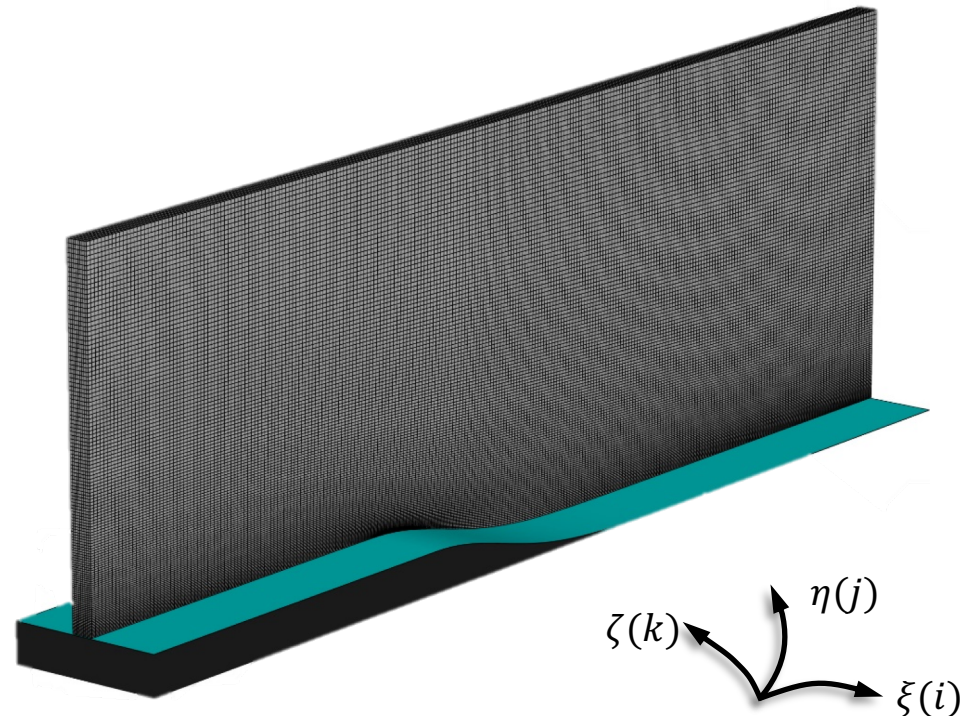
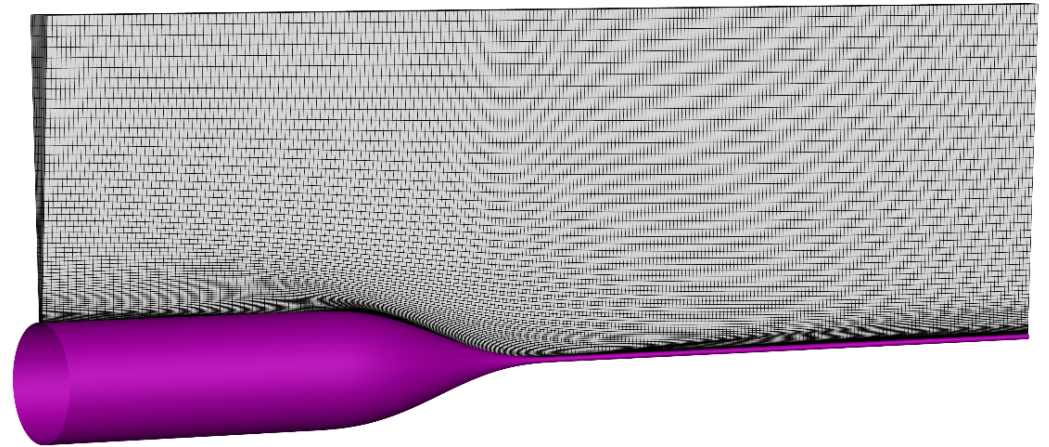
We pursue this approach!

Orthogonal grid generation

- Orthogonal grid is generated by solving a *coupled system of non-linear Poisson equations* (Eça, *JCP* 1996)

- 2D: $g_{12} = 0 \Rightarrow$
$$\frac{\partial}{\partial \xi} \left(\frac{h_\eta}{h_\xi} \frac{\partial x}{\partial \xi} \right) + \frac{\partial}{\partial \eta} \left(\frac{h_\xi}{h_\eta} \frac{\partial x}{\partial \eta} \right) = 0$$
$$\frac{\partial}{\partial \xi} \left(\frac{h_\eta}{h_\xi} \frac{\partial y}{\partial \xi} \right) + \frac{\partial}{\partial \eta} \left(\frac{h_\xi}{h_\eta} \frac{\partial y}{\partial \eta} \right) = 0$$

- We added:
 - **Grid stretching in wall-normal direction** (Ferrante & Elghobashi, *JCP* 2004)
 - **Grid stretching also in the stream-wise direction**
 - Stream-wise discretization of the bottom boundary performed on the basis of **constant arc-length**



Pressure-correction method for NS in *orthogonal* curvilinear coordinates

- Governing equations in orthogonal coordinates ($g = |g_{ij}|$):

$$\frac{1}{\sqrt{g}} \left[\frac{\partial}{\partial \xi} (\sqrt{g} \hat{U}) + \frac{\partial}{\partial \eta} (\sqrt{g} \hat{V}) + \frac{\partial}{\partial \zeta} (\sqrt{g} \hat{W}) \right] = 0$$

$$\frac{\partial \hat{U}^i}{\partial t} + (\text{conv})^i = -\frac{1}{\rho} (\text{pres})^i + (\text{visc})^i$$

← “Stiff”

- Spatial discretization
 - 2nd order central difference scheme on staggered grid
- FFT-based fast Poisson solver for pressure in orthogonal coordinates (**FastPoc**)
- A simple choice for time-integration like 2nd order Adams-Bashforth gives **loss of temporal accuracy** (to 1st order) for **wall-bounded flows**

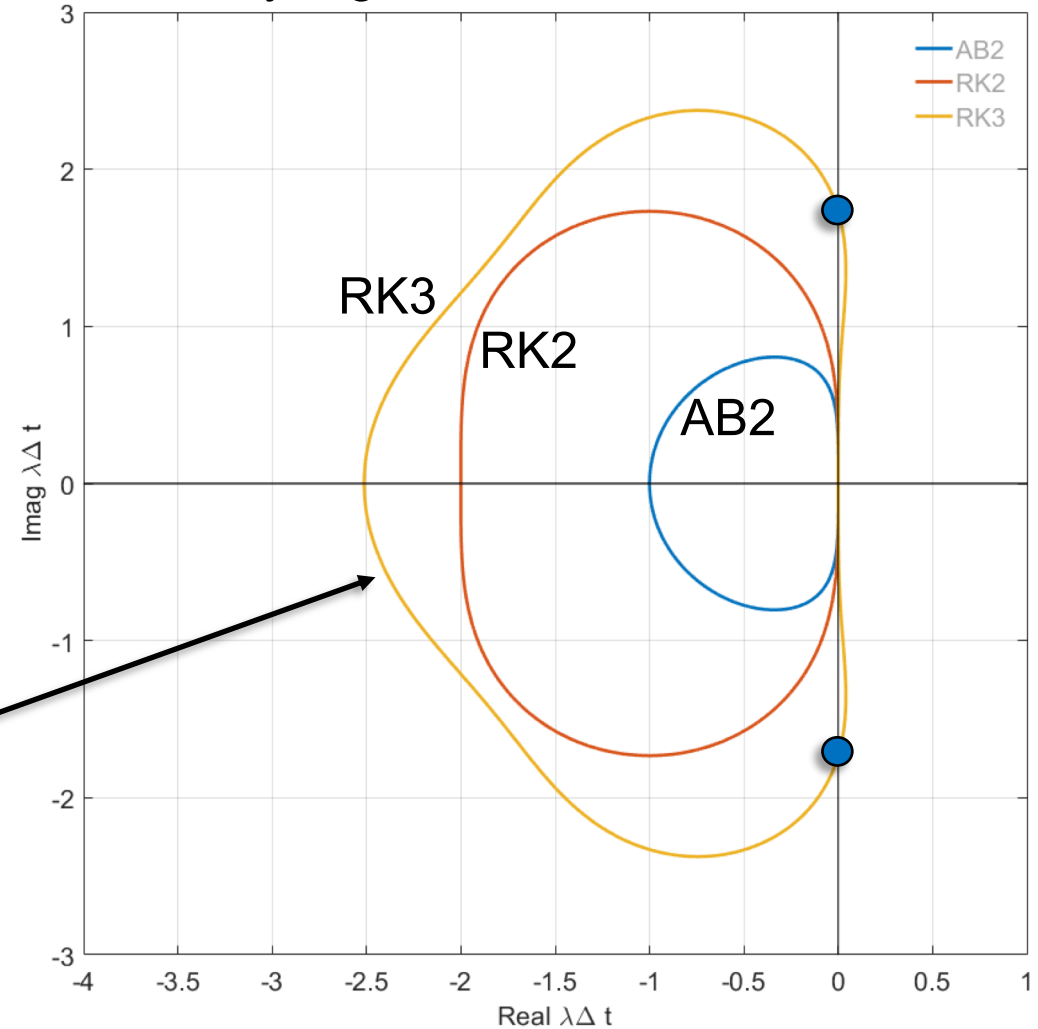
We need a different scheme for *time-integration*!

Time integration scheme

- **AB2 & RK2**
 - unconditionally unstable for pure convection
 - smaller stability region than RK3
- **RK3**
 - Theoretical CFL limit for pure convection is $\sqrt{3}$
 - **Larger stability zone**

We use RK3
for time integration

Stability regions for AB2, RK2 & RK3



Standard RK3

Discrete operator: $R(\mathbf{U}) = -\nabla \cdot (\mathbf{U}\mathbf{U}) + \nu \nabla^2 \mathbf{U}$

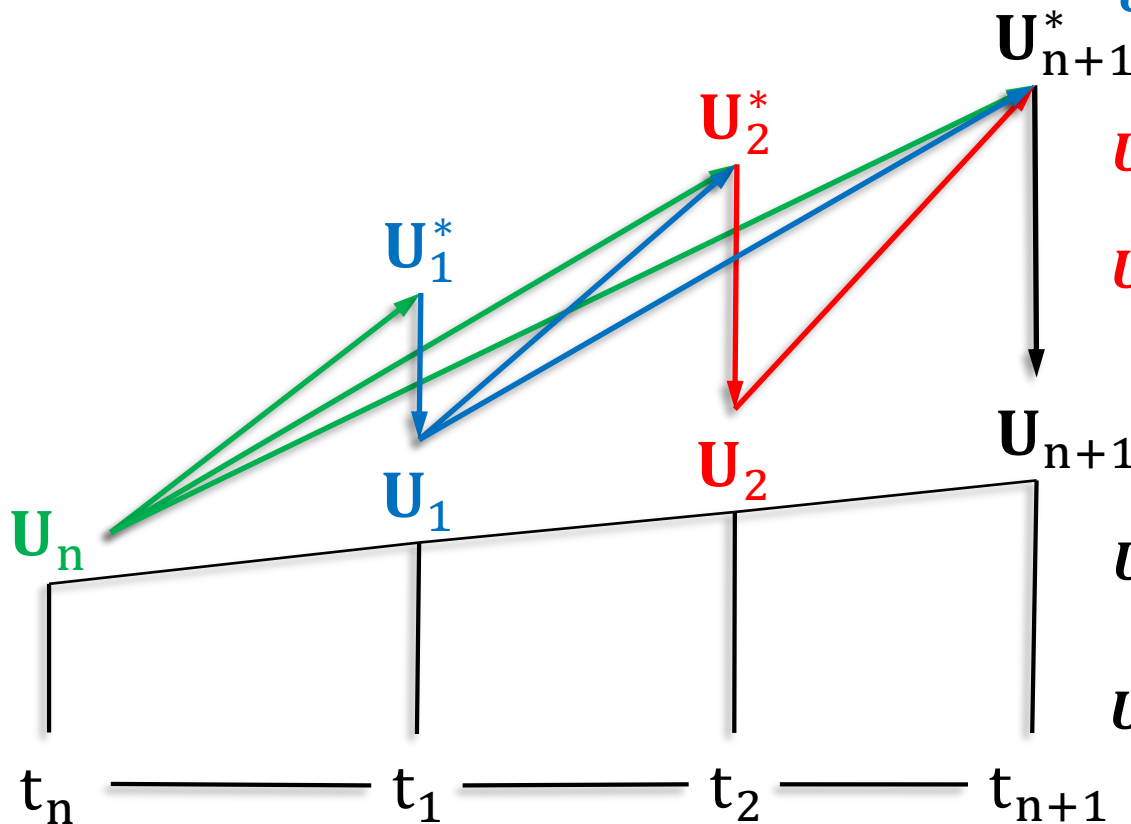
NS equation: $\frac{\partial \mathbf{U}}{\partial t} = -\nabla \phi + R(\mathbf{U})$

$$\mathbf{U}_1^* = \mathbf{U}_n + \frac{\Delta t}{3} R(\mathbf{U}_n)$$

$$\mathbf{U}_1 = \mathbf{U}_1^* - \frac{\Delta t}{3} \nabla \phi_1$$

$$\mathbf{U}_2^* = \mathbf{U}_n + \Delta t [-R(\mathbf{U}_n) + 2R(\mathbf{U}_1)]$$

$$\mathbf{U}_2 = \mathbf{U}_2^* - \Delta t \nabla \phi_2$$



$$\mathbf{U}_{n+1}^* = \mathbf{U}_n + \Delta t \left[\frac{3}{4} R(\mathbf{U}_1) + \frac{1}{4} R(\mathbf{U}_2) \right]$$

$$\mathbf{U}_{n+1} = \mathbf{U}_{n+1}^* - \Delta t \nabla \phi_{n+1}$$

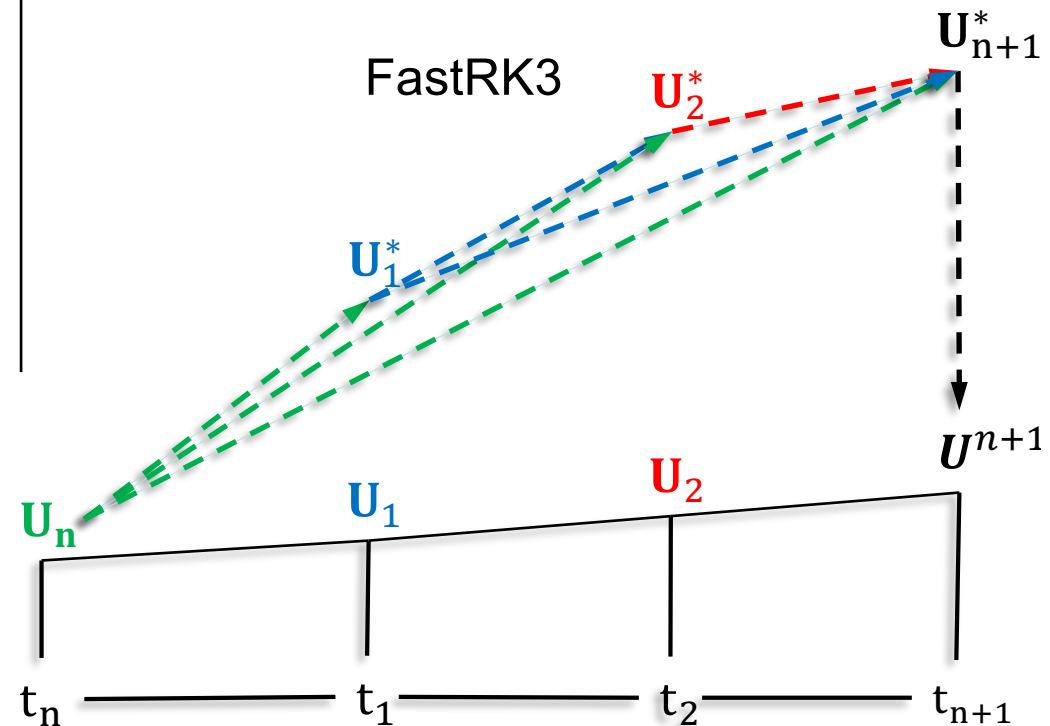
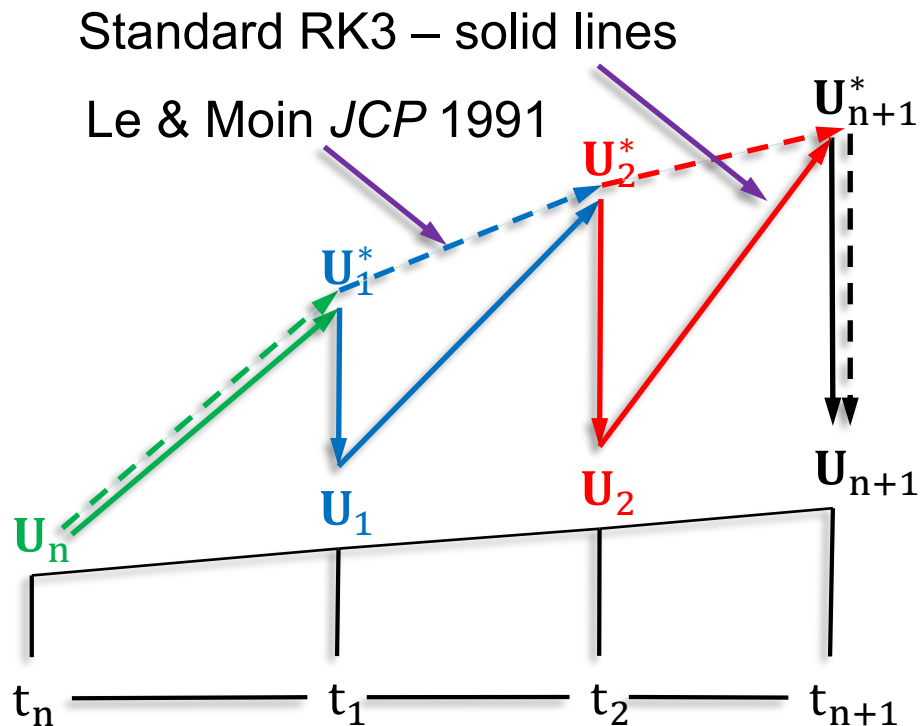
Time integration scheme

Le & Moin <i>JCP</i> 1991	Present: FastRK3
Convective (nonlinear): <i>Explicit</i>	Convective (nonlinear): <i>Explicit</i>
Diffusive (linear): <i>Implicit</i>	Diffusive (linear): <i>Explicit</i>
Temporal convergence rate: 2nd order	Temporal convergence rate: 3rd order

Semi-Implicit & 2nd order

Explicit & 3rd order

Still only one Poisson eq solved

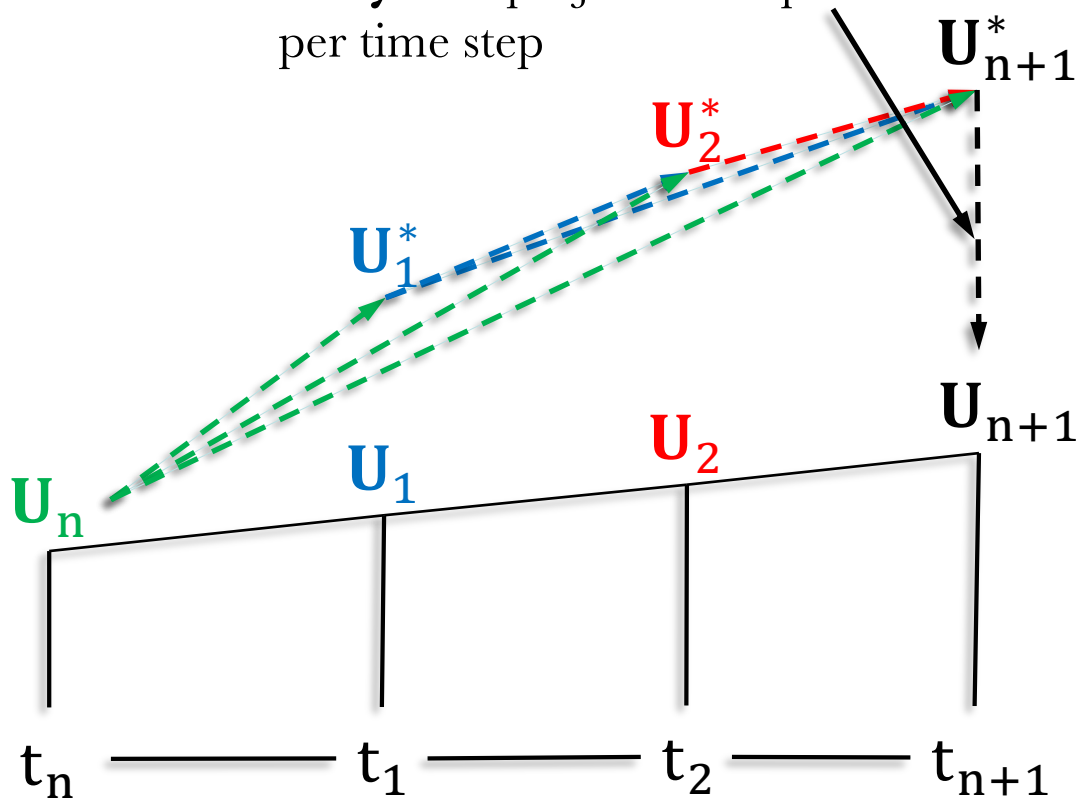


FastRK3

$$\frac{\partial U}{\partial t} = -\nabla\phi + R(U)$$

$$R(U) = -\nabla \cdot (UU) + \nu\nabla^2 U$$

Only one projection step
per time step



(A1) Compute: $U_1^* = U_n + \frac{\Delta t}{3} R(U_n)$

(A2) Substitute: $U_1 = U_1^* - \frac{\Delta t}{3} \nabla\phi_1 \Rightarrow$

$$U_2^* = U_n + \Delta t \left[\begin{array}{c} -R(U_n) \\ +2R\left(U_1^* - \frac{\Delta t}{3} \nabla\phi_1\right) \end{array} \right]$$

(A3) Substitute: $U_2 = U_2^* - \Delta t \nabla\phi_2 \Rightarrow$

$$U_{n+1}^* = U_n + \Delta t \left[\begin{array}{c} \frac{3}{4} R\left(U_1^* - \frac{\Delta t}{3} \nabla\phi_1\right) \\ +\frac{1}{4} R(U_2^* - \Delta t \nabla\phi_2) \end{array} \right]$$

(B) $\nabla^2\phi_{n+1} = \frac{\rho}{\Delta t} \nabla \cdot U_{n+1}^*$

(C) $U_{n+1} = U_{n+1}^* - \Delta t \nabla\phi_{n+1}$

FastRK3 (cont.)

- We need to compute $\Delta t \nabla \phi_1$ and $\Delta t \nabla \phi_2$!
- Le & Moin, *JCP* (1991) used constant extrapolation:

$$\begin{aligned}\Delta t \nabla \phi_1 &= \Delta t [\nabla \phi_n] + O(\Delta t^2) \\ \Delta t \nabla \phi_2 &= \Delta t [\nabla \phi_n] + O(\Delta t^2)\end{aligned}$$

LM is second-order accurate

- We perform linear extrapolation in time:

$$\begin{aligned}\Delta t \nabla \phi_1 &= \Delta t \left[\frac{2}{3} \nabla \phi_n - \frac{1}{3} \nabla \phi_{n-1} \right] + O(\Delta t^3) \\ \Delta t \nabla \phi_2 &= \Delta t [2 \nabla \phi_n - \nabla \phi_{n-1}] + O(\Delta t^3)\end{aligned}$$

We preserve third-order accuracy

Convergence study: Stokes 1st problem

- Sudden acceleration of an infinite plate to constant U_∞
- Momentum eq reduces to a **pure diffusion equation**

$$\frac{\partial U}{\partial t} = \nu \frac{\partial^2 U}{\partial y^2}$$

- BC's

1. $U = 0$ for all y at $t = 0$
2. $U = 0$ for all t as $y \rightarrow \infty$
3. $U = U_\infty$ at $y = 0$ for $t > 0$

- Solution

$$U(y, t) = U_\infty \operatorname{erfc}(\eta) \text{ where } \eta = \frac{y}{2\sqrt{\nu t}}.$$

Convergence study: Stokes 1st problem

Flat plate and cylinder

$$t = 5s, \nu = 10^{-4} \text{ m}^2/s$$

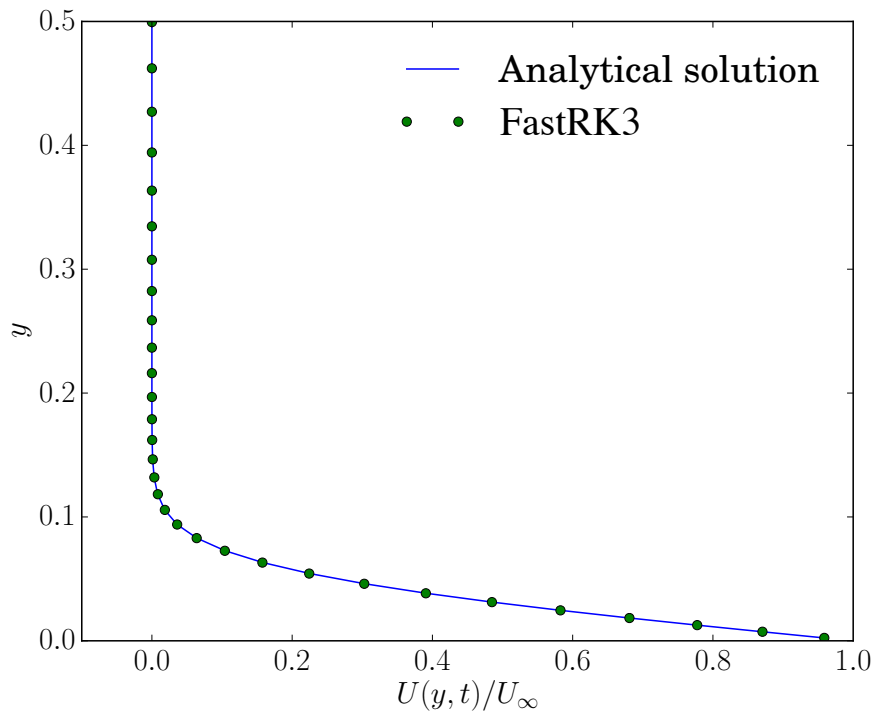
$$\Delta t_{c_{max}} = \sqrt{3} \frac{\Delta x}{U_{\infty}} = 0.07s$$

$$\Delta t_{v_{max}} \approx \frac{5\Delta y^2}{8\nu} = 0.13s$$

[Hirsch 2007]

Analytically, the momentum equation reduces to a **pure diffusion equation**

Present method is 3rd order accurate in time



Flat plate

	$E_{4\Delta t, 2\Delta t}$	$E_{2\Delta t, \Delta t}$	Rate
$U(y, t)$	3.0×10^{-6}	3.4×10^{-7}	3.1

Flat plate

	$E_{4\Delta t, 2\Delta t}$	$E_{2\Delta t, \Delta t}$	Rate
$U(r, t)$	4.6×10^{-3}	5.1×10^{-4}	3.2

Cylinder

The discrete Poisson operator

- Coordinate transformation results in a *variable coefficient Poisson equation* that is solved using FFT-based method – FastPoc

$$(B) \nabla^2 \phi_{n+1} = \frac{\rho}{\Delta t} \nabla \cdot \mathbf{U}_{n+1}^*$$

$$f_1(\xi, \eta, \zeta) \left[\frac{\partial}{\partial \xi} \left(f_2(\xi, \eta, \zeta) \frac{\partial \phi}{\partial \xi} \right) + \frac{\partial}{\partial \eta} \left(f_3(\xi, \eta, \zeta) \frac{\partial \phi}{\partial \eta} \right) + \frac{\partial}{\partial \zeta} \left(f_4(\xi, \eta, \zeta) \frac{\partial \phi}{\partial \zeta} \right) \right] = \frac{\rho}{\Delta t} (\nabla \cdot \mathbf{U}_{n+1}^*)$$

- Orthogonality of grid ensures **no cross-derivates** are present
- Discrete Poisson operator (2nd order central difference) is a **Symmetric Positive-Definite** matrix with 7 non-zero diagonals
- At least **one direction of homogeneity** due to the nature of grids employed:

$$f_1(\xi, \eta) \left[\frac{\partial}{\partial \xi} \left(f_2(\xi, \eta) \frac{\partial \phi}{\partial \xi} \right) + \frac{\partial}{\partial \eta} \left(f_3(\xi, \eta) \frac{\partial \phi}{\partial \eta} \right) + f_4(\xi, \eta) \frac{\partial^2 \phi}{\partial \zeta^2} \right] = \frac{\rho}{\Delta t} (\nabla \cdot \mathbf{U}_{n+1}^*)$$

FastPoc algorithm: FFT-based parallel Poisson solver for orthogonal curvilinear coordinates

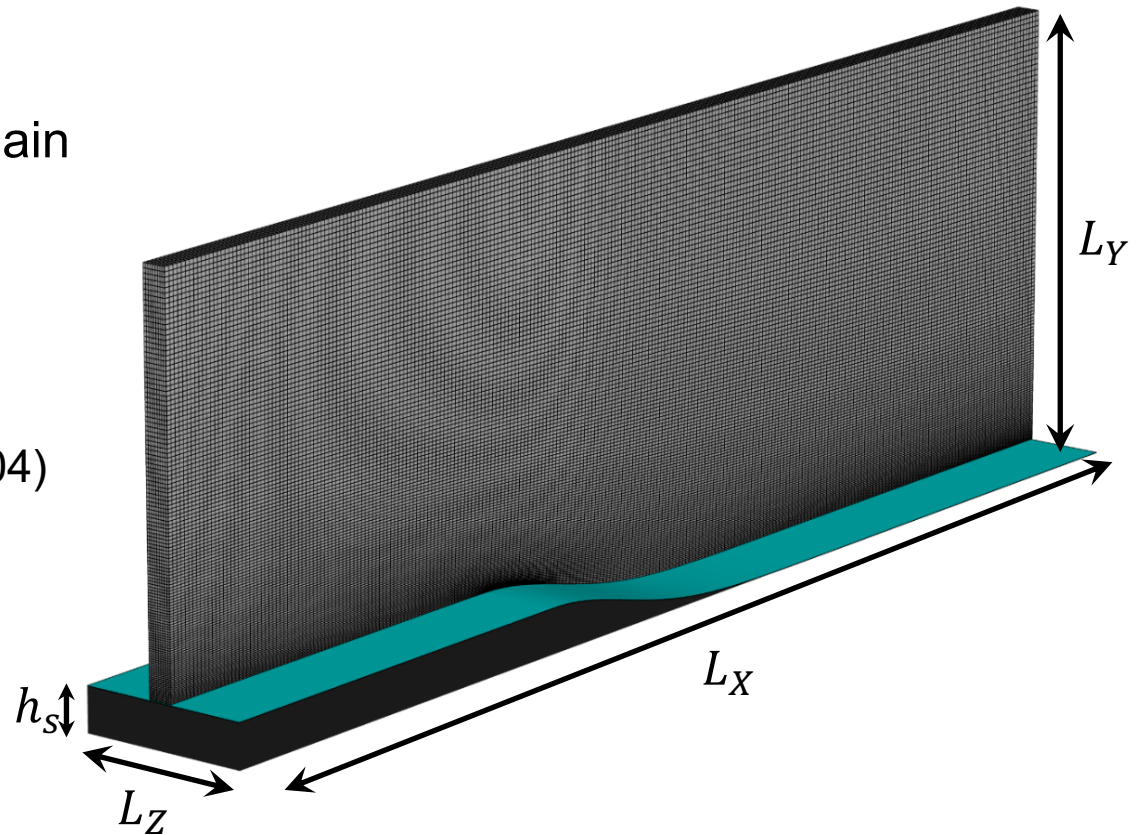
1. Perform real-to-complex **FFT along the direction of homogeneity** [ζ -direction (k)] to obtain **2D block-tridiagonal complex-valued** systems of size $N_I \times N_J$
2. Solve the resulting 2D complex systems for each $i - j$ plane using **LDL^T decomposition**
3. Perform complex-to-real **inverse FFT** in ζ -direction

(We have used MPI, FFTW, all-to-all zero-copy transpose method, and fill-in reducing nested dissection ordering)

Scalability of FastPoc: Flow over curved ramp

- Two cases with the same domain and grid size

$N_X \times N_Y \times N_Z = 1024 \times 256 \times 512$
 $(L_X, L_Y, L_Z) = (20h_s, 5h_s, 5h_s)$
 but different grid stretching γ
 (Ferrante & Elghobashi, *JCP* 2004)

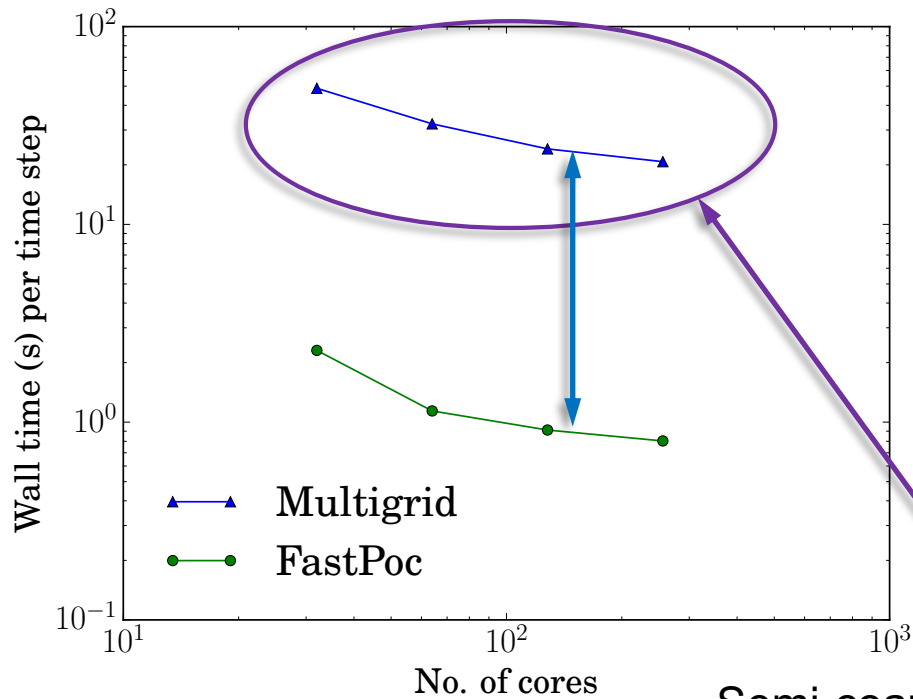


	γ	y_{min}/h_s	$y_{min}^+ \dagger$
Case A	0.33	5.9×10^{-3}	3.8
Case B	0.66	8.4×10^{-4}	0.3

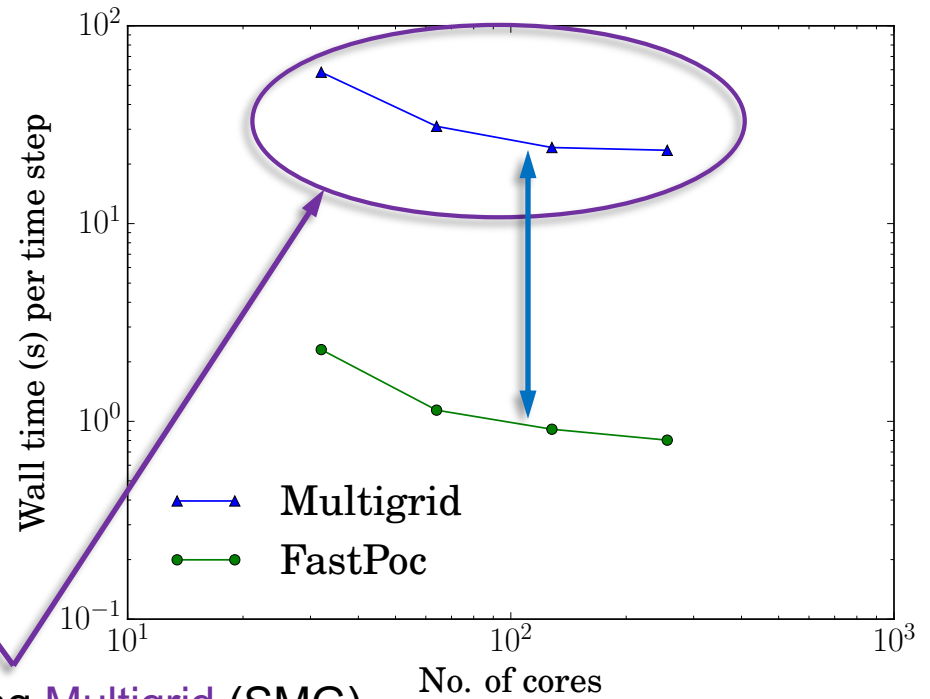
$\dagger Re_\delta = 8000$

Comparison of wall time of Multigrid vs FastPoc

Case A: $\gamma = 0.33$



Case B: $\gamma = 0.66$



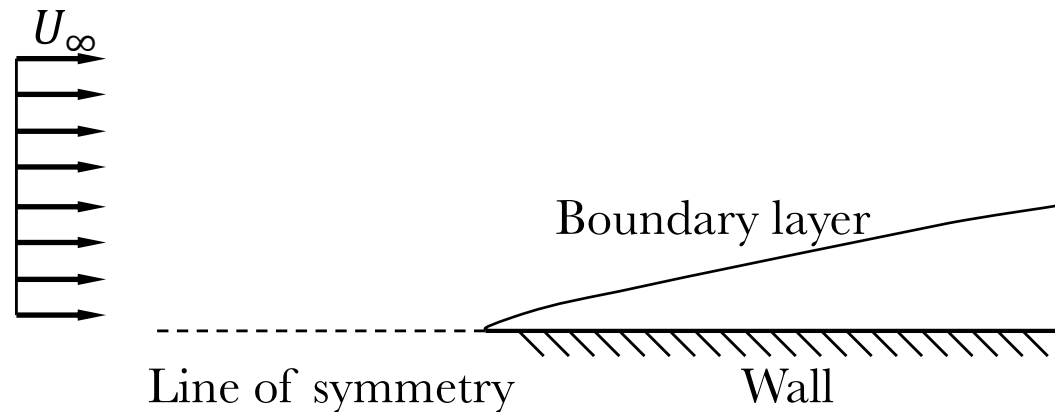
Semi-coarsening Multigrid (SMG)
performance depends on grid
stretching

Multigrid tolerance	Multigrid (s)	FastPoc (s)	Speedup
$ \nabla \cdot \mathbf{U}^{n+1} _{max} < 10^{-6}$	23.5 (4 iter.)	0.8	29
$ \nabla \cdot \mathbf{U}^{n+1} _{max} < 10^{-12}$	48 (12 iter.)	0.8	60

	Total memory
Multigrid	336 GB
FastRK3	342 GB

Verification case: Laminar flow over flat plate

Uniform inlet



Similarity solutions as function of similarity variable $\eta(x, y)$,

$$f'(\eta) = \frac{U(\eta)}{U_\infty}; \quad \eta = \frac{y\sqrt{Re_x}}{x}; \quad Re_x = \frac{U_\infty x}{\nu};$$

which satisfies:

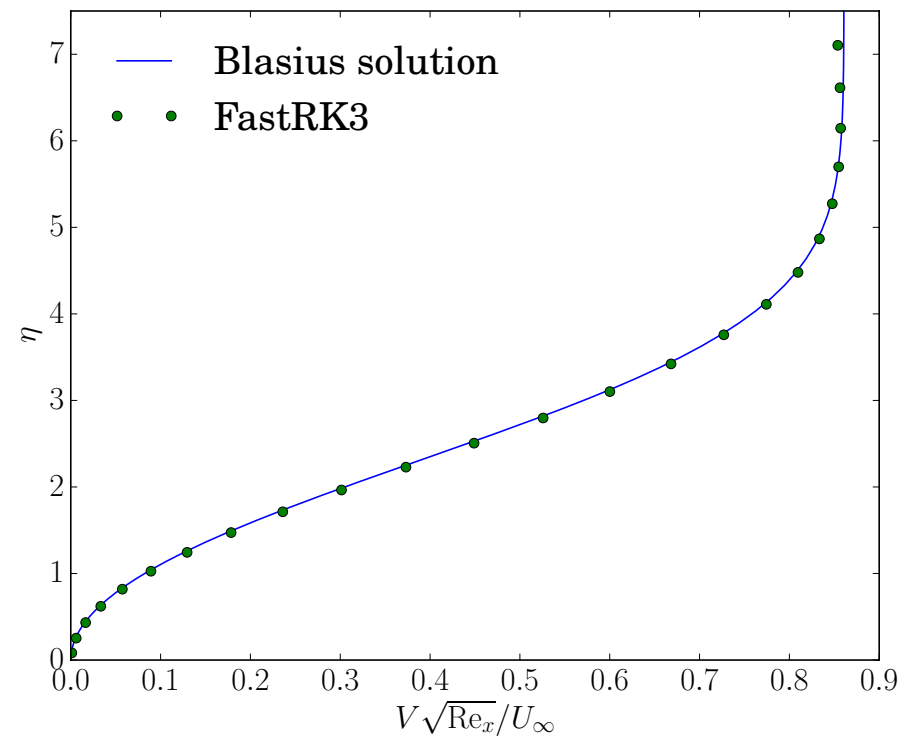
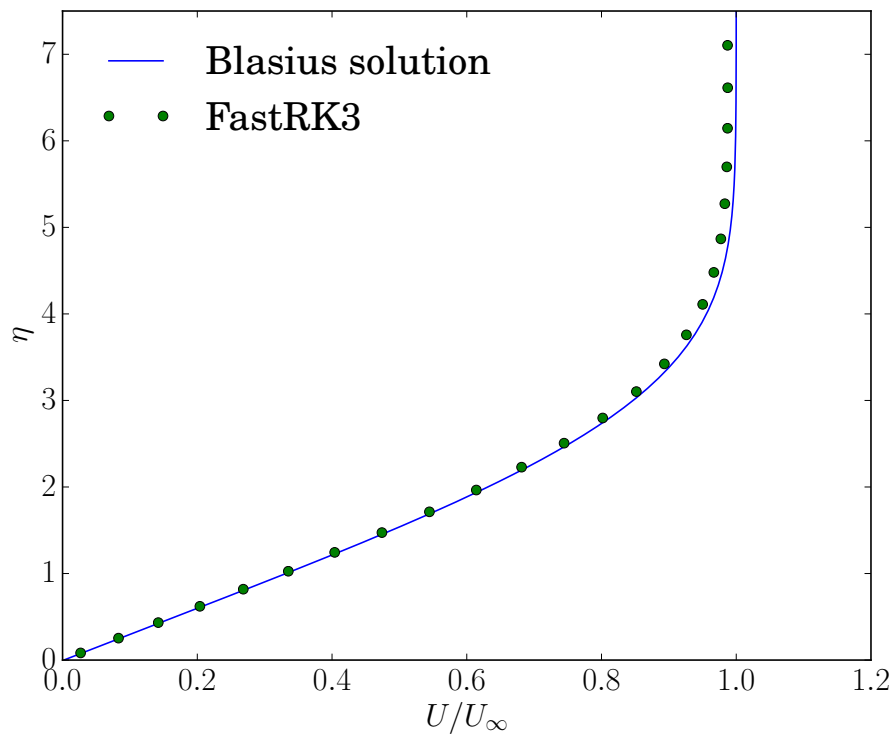
$$2f''' + ff' = 0,$$

with BC's: $f'(0) = 0$, $f'(\infty) = 0$, $f(0) = 0$. The velocity components are:

$$U(x, y) = U_\infty f'(\eta),$$
$$V(x, y) = -\frac{U_\infty}{2\sqrt{Re_x}} (f(\eta) - \eta f'(\eta)).$$

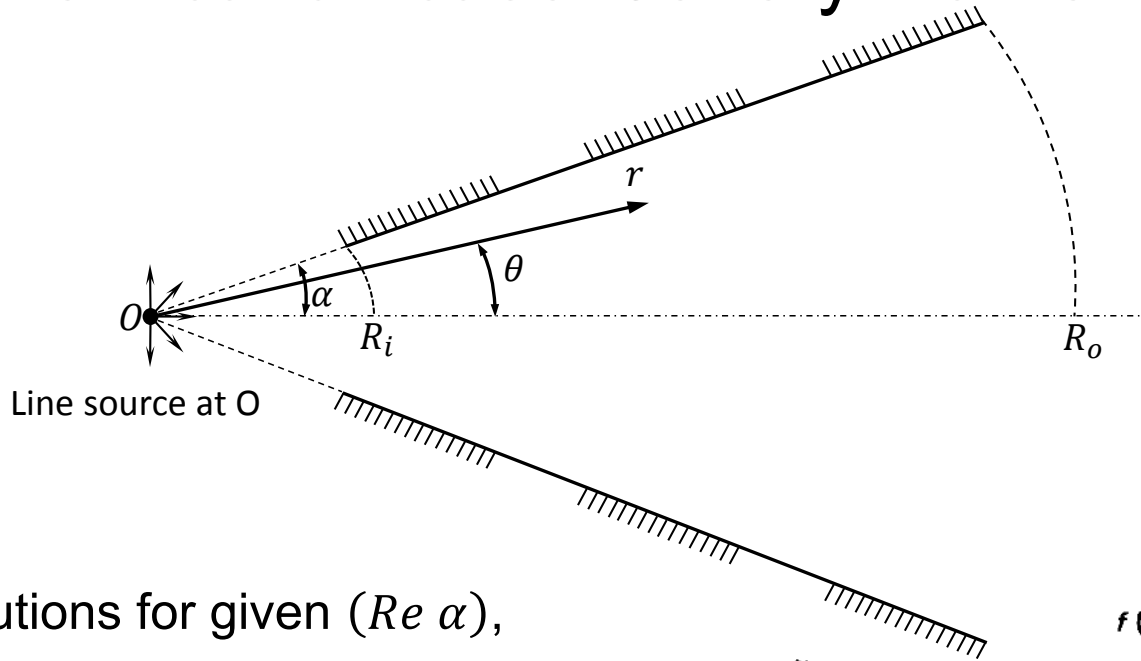
Verification: Laminar flow over flat plate

L_x	L_y	L_z	Re_x
10	3.6	5	357



	$E_{4\Delta y, 2\Delta y}$	$E_{2\Delta y, \Delta y}$	Rate
U	1.5e-2	3.8e-3	1.9
V	4.5e-1	1.1e-1	2.0

Verification case: Jeffery-Hamel flow



Similarity solutions for given $(Re \alpha)$,

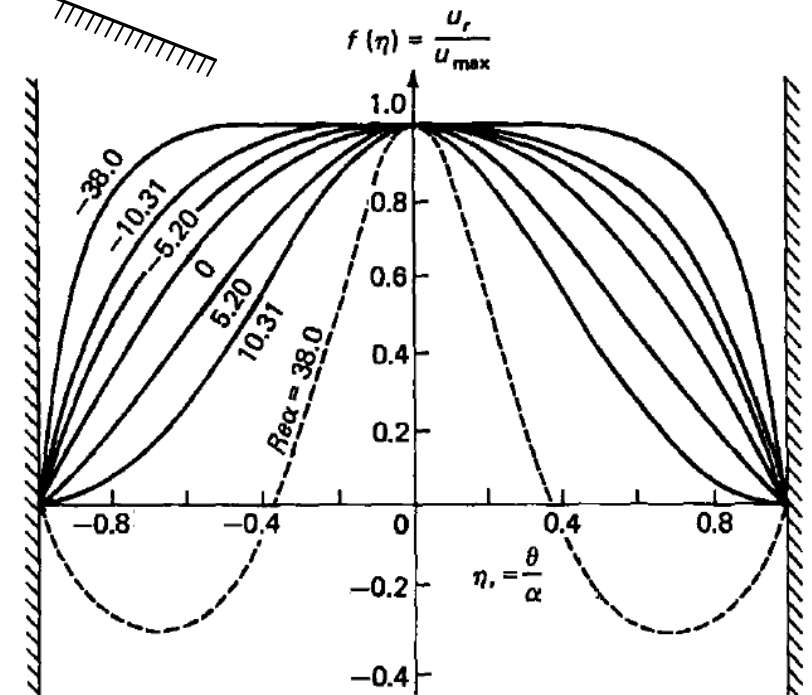
$$f(\eta) = \frac{U_r(\eta)}{U_{max}}; \quad \eta = \frac{\theta}{\alpha}; \quad U_{max} = U_{max}(r) \propto 1/r$$

which satisfies:

$$f'''' + 2(Re \alpha) f f' + 4\alpha^2 f' = 0$$

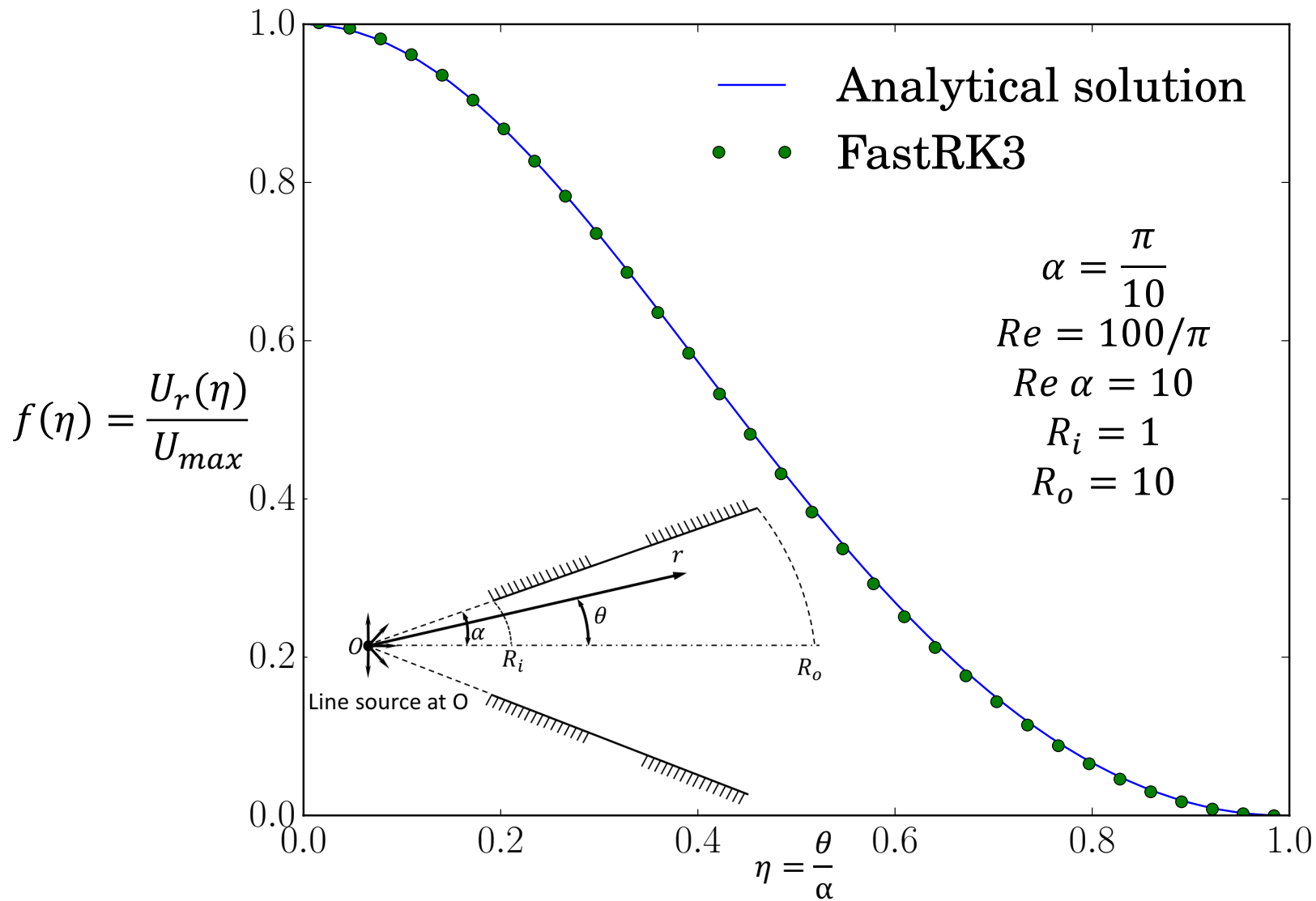
with BC's: $f(\pm 1) = 0, f(0) = 1$

where, $Re = \frac{U_{max} r \alpha}{\nu}$



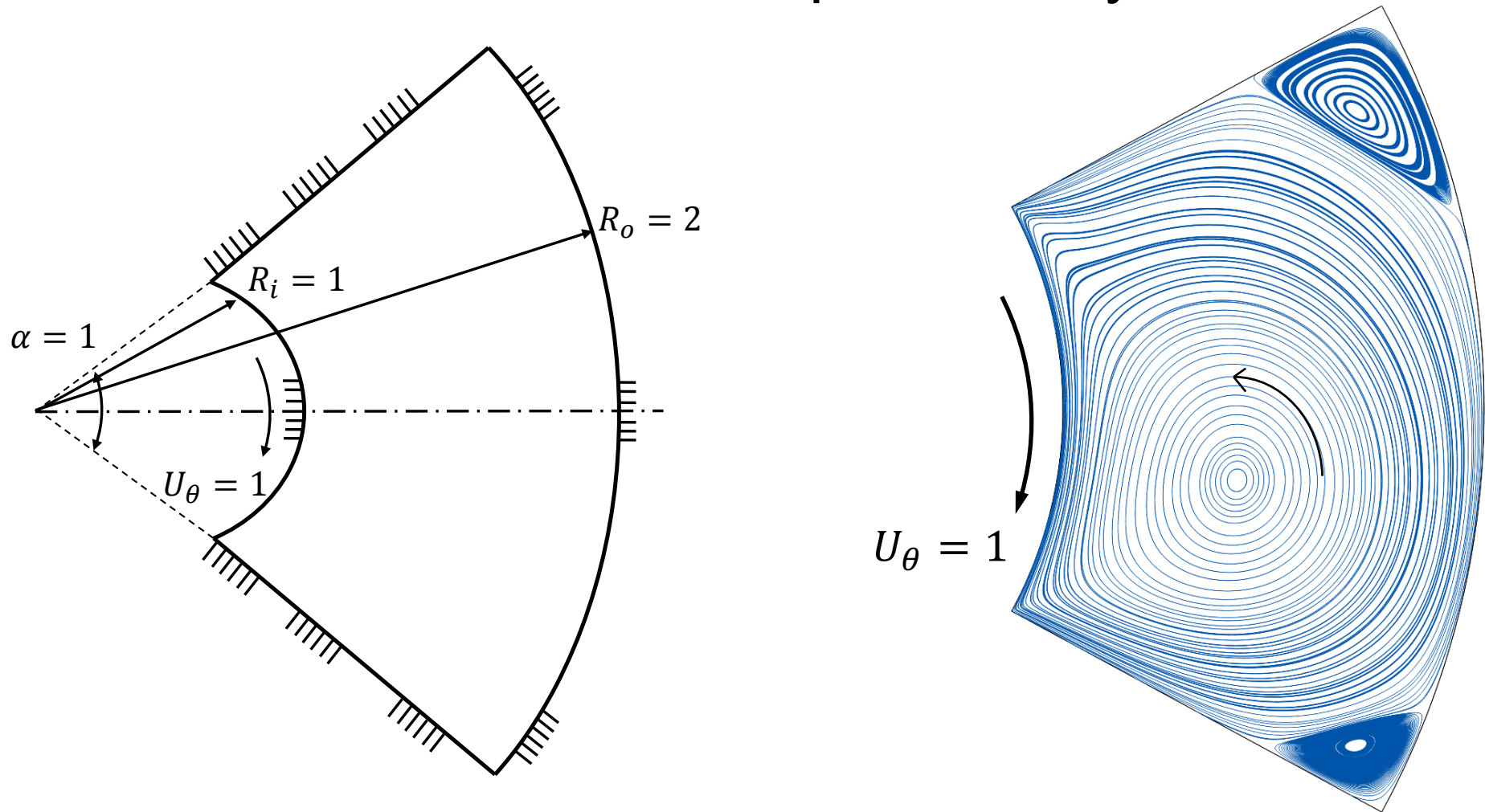
(White 1974)

Verification: Jeffery-Hamel flow



	$E_{4\Delta\theta, 2\Delta\theta}$	$E_{2\Delta\theta, \Delta\theta}$	Rate
U_r	1.9×10^{-2}	4.6×10^{-3}	2.0
p	1.1×10^{-4}	2.2×10^{-5}	2.3

Validation: Driven polar-cavity flow

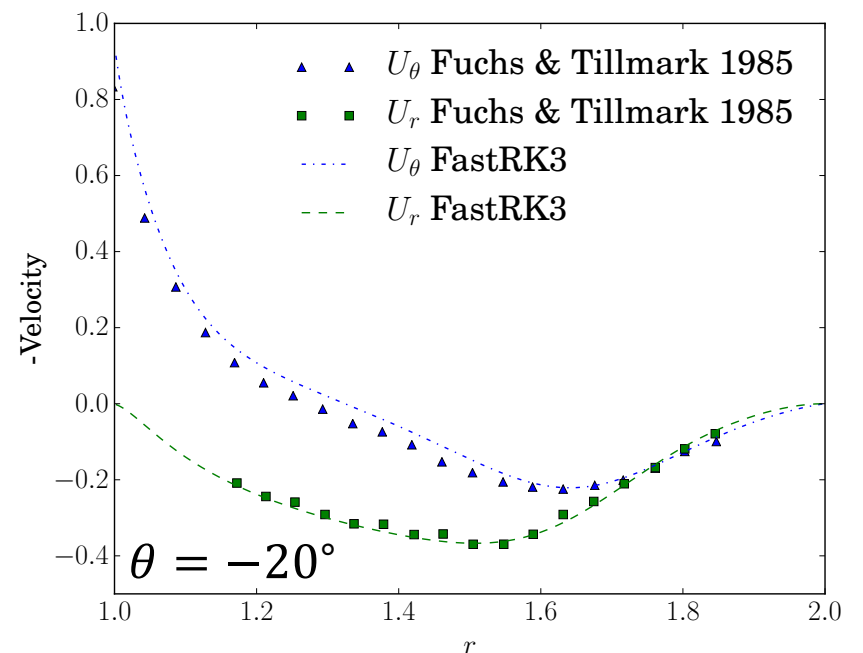
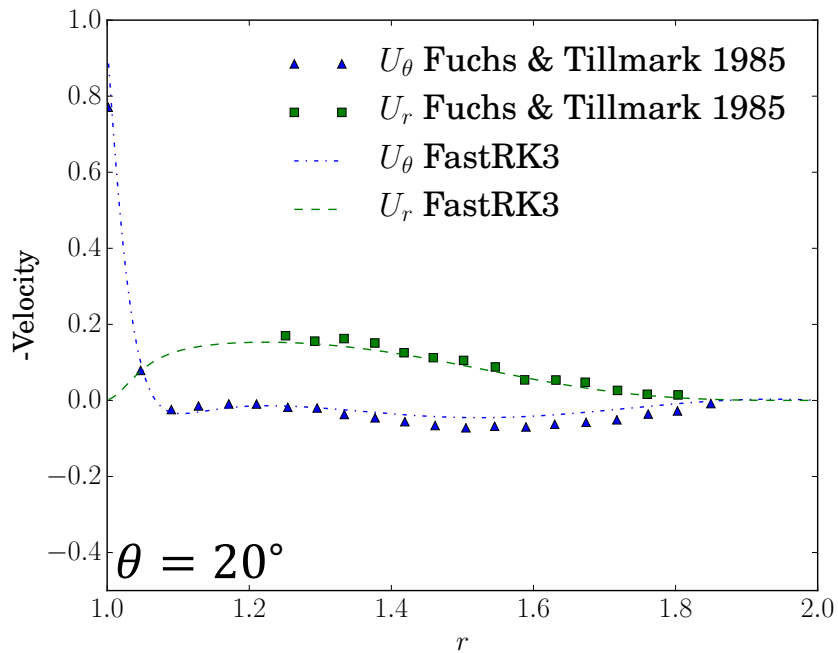
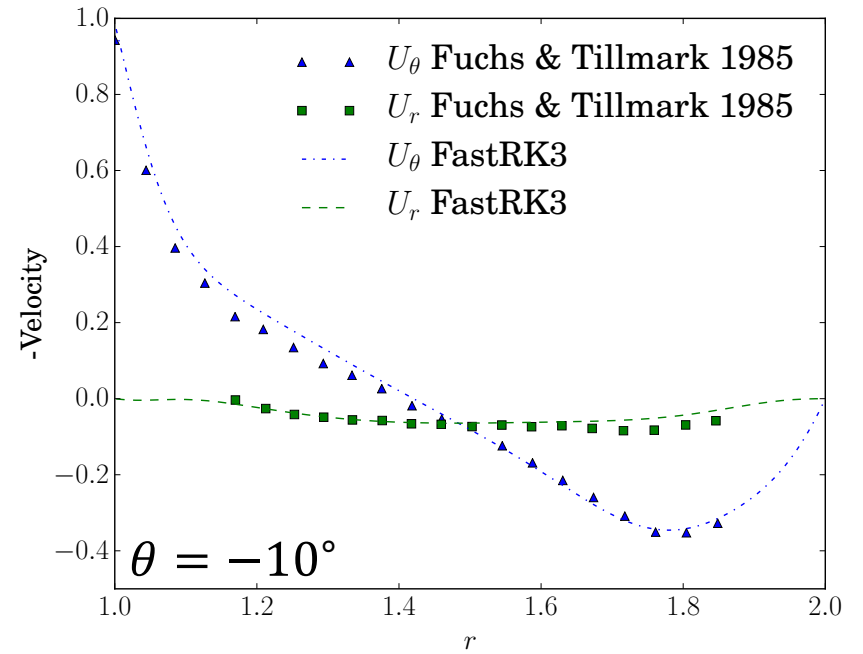
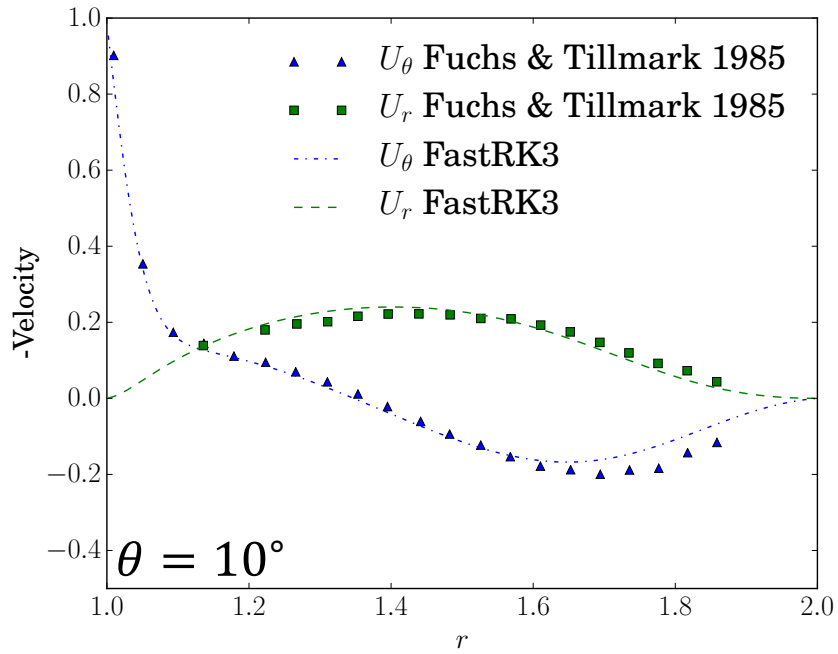


Experiments by Fuchs & Tillmark 1985

Reynolds number: $Re_i = 350$

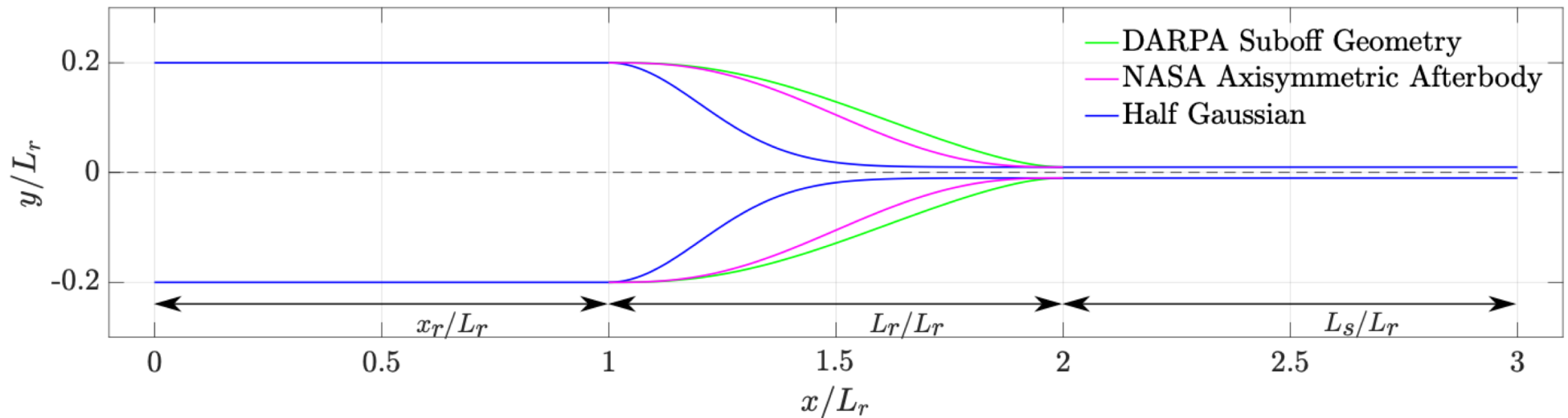
Grid size: 256×192

Validation: Driven polar-cavity flow

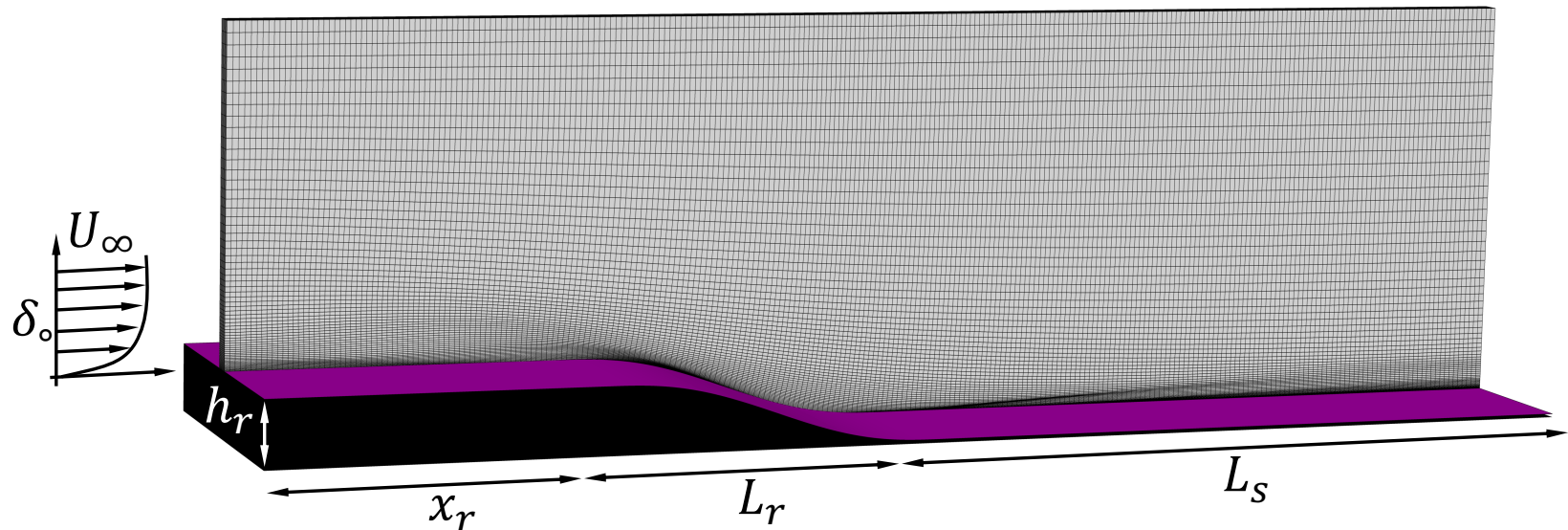


Application: flow over curved ramps

- Three ramp profiles
 1. DARPA Suboff geometry (Groves et. al. 1989)
 2. NASA axisymmetric afterbody (Disotell & Rumsey 2017)
 3. Half Gaussian



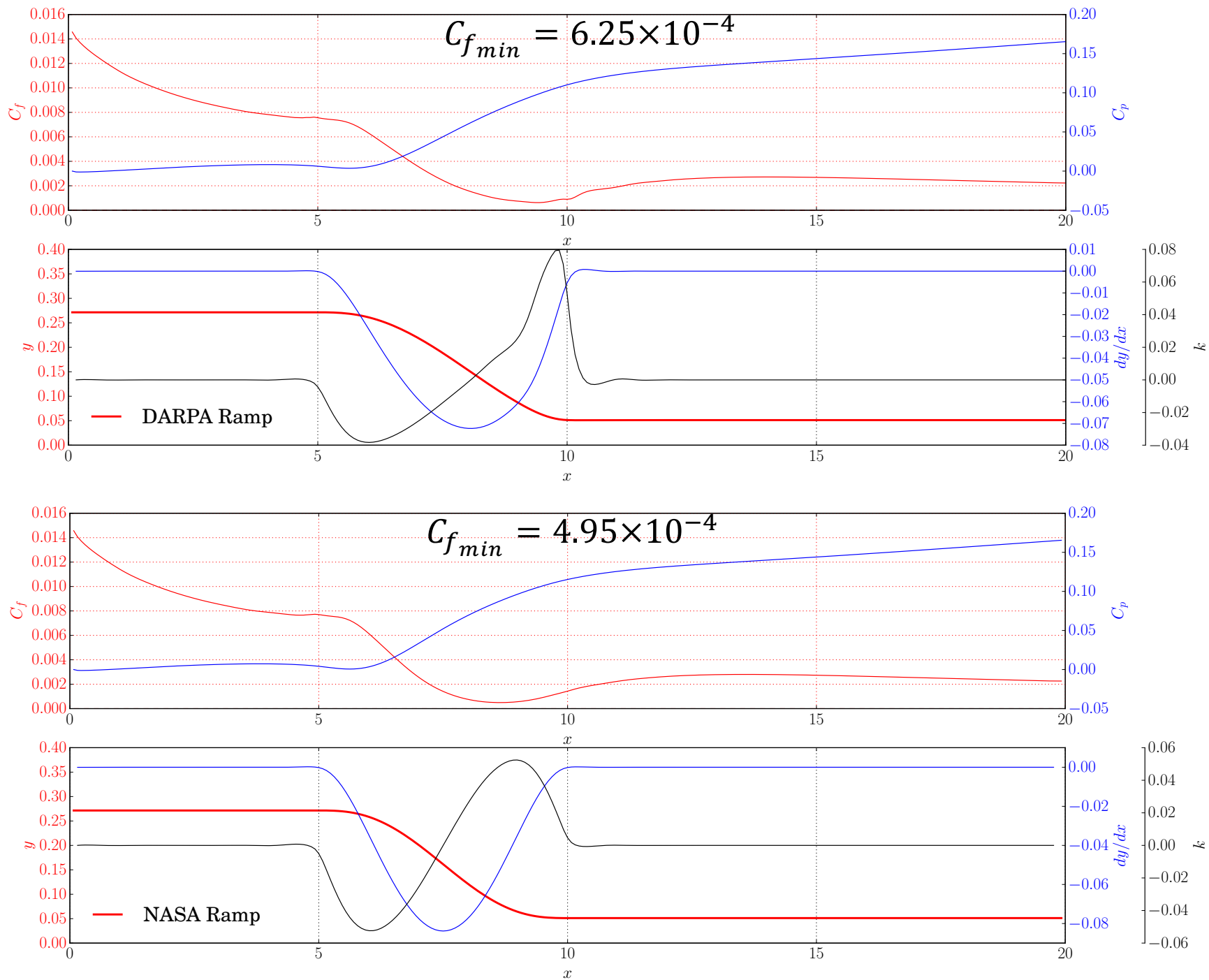
Flow over curved ramps



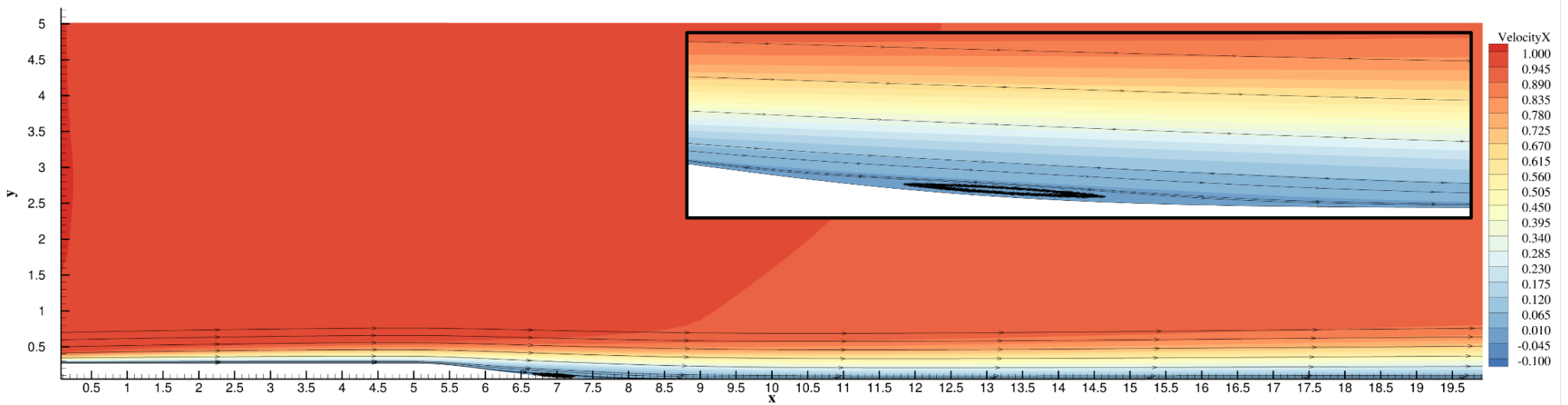
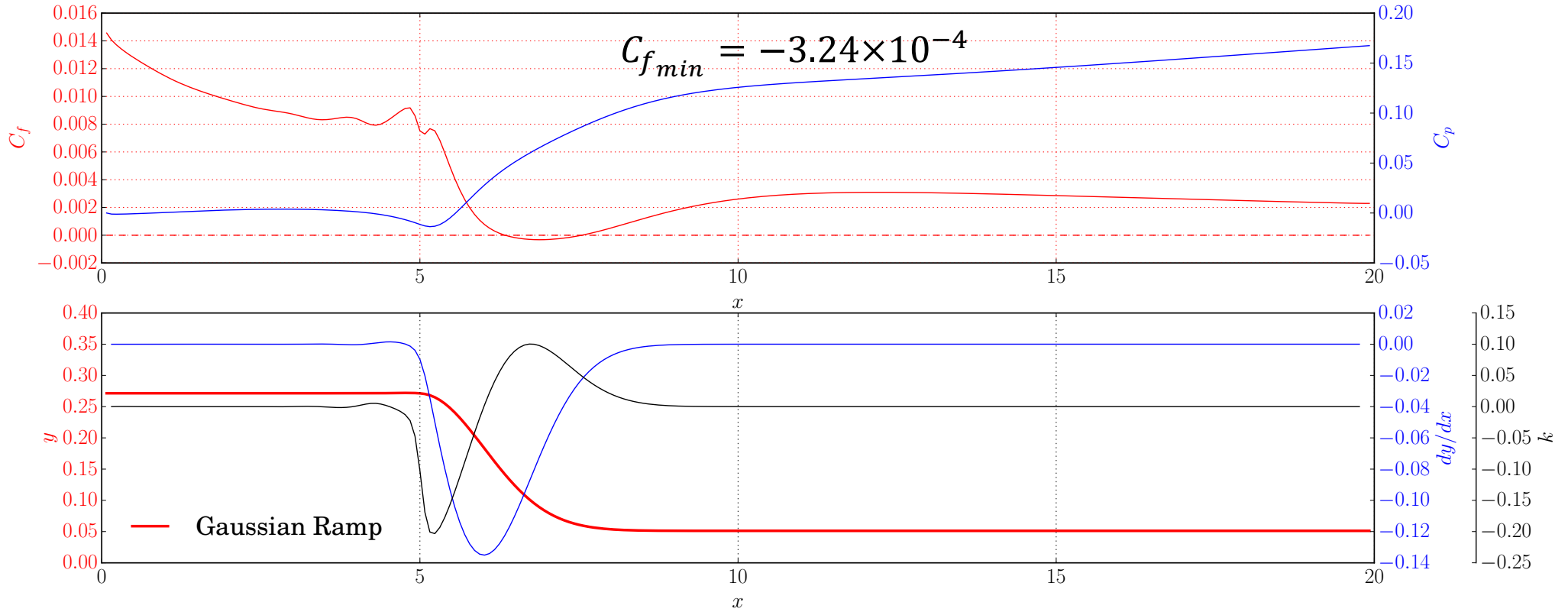
- $Re_{L_r} = 5000$
- $h_r = 0.054L_r \Rightarrow Re_{h_r} = 270$
- $\delta_o = 0.004L_r$
- $x_r = L_r$
- $L_s = 2L_r$
- $256 \times 64 \times 128$

- Same dimensions and inlet conditions for the three ramp profiles
- Identify dimensions which result in attached and separated flows

Flow over curved ramps

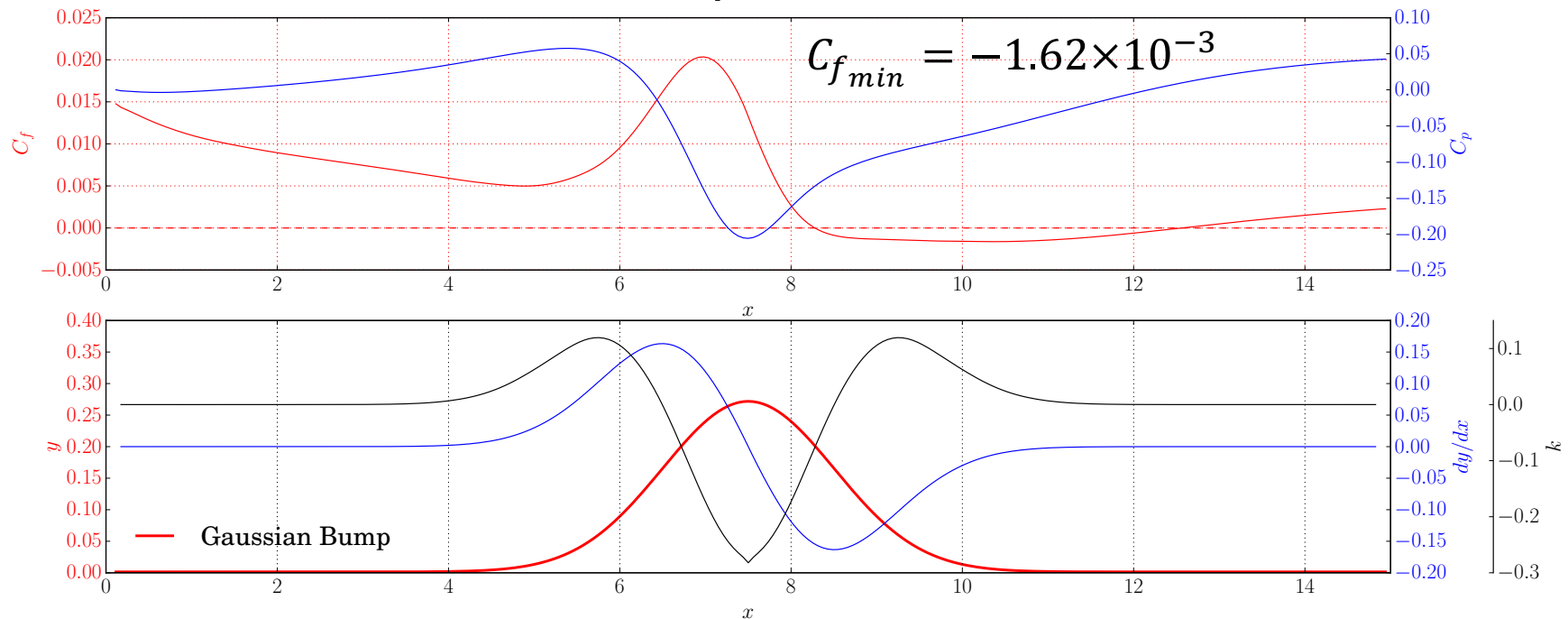
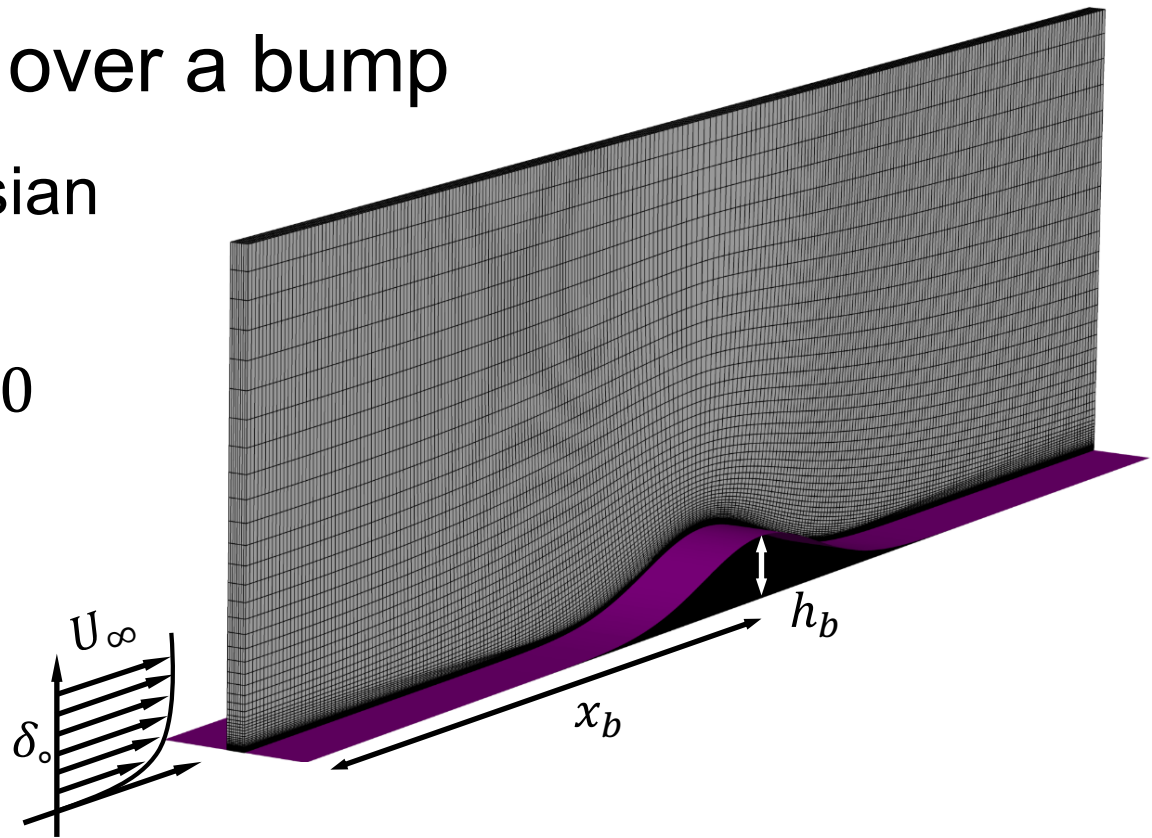


Flow over curved ramps

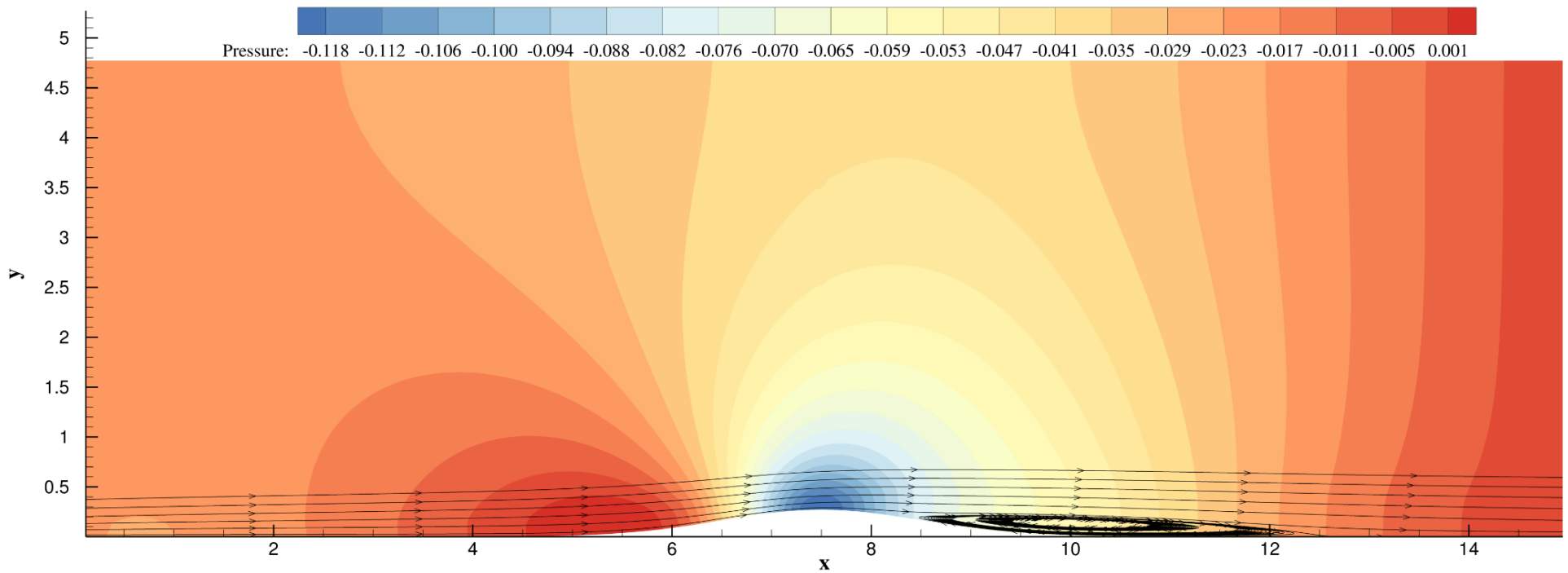
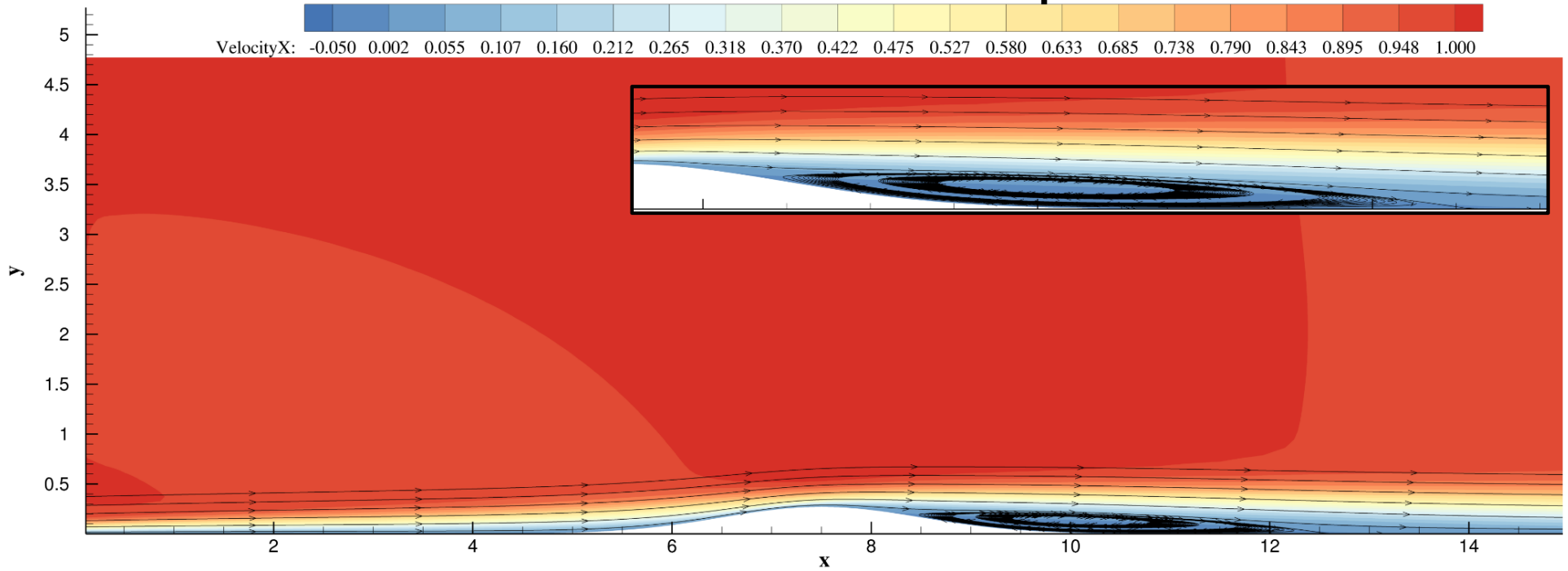


Flow over a bump

- $L_b = 5\sigma$, std. dev of Gaussian
- $x_b = 1.5L_b$
- $h_b = 0.054L_b \Rightarrow Re_{h_b} = 270$
- $\delta_o = 0.004L_b$
- $Re_{L_b} = 5000$
- Similar dimensions as the curved ramps



Flow over a bump

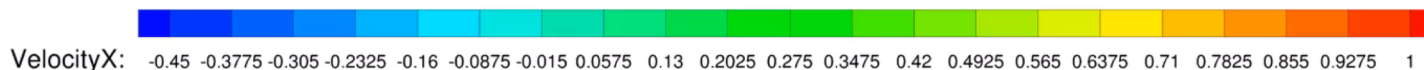


Summary

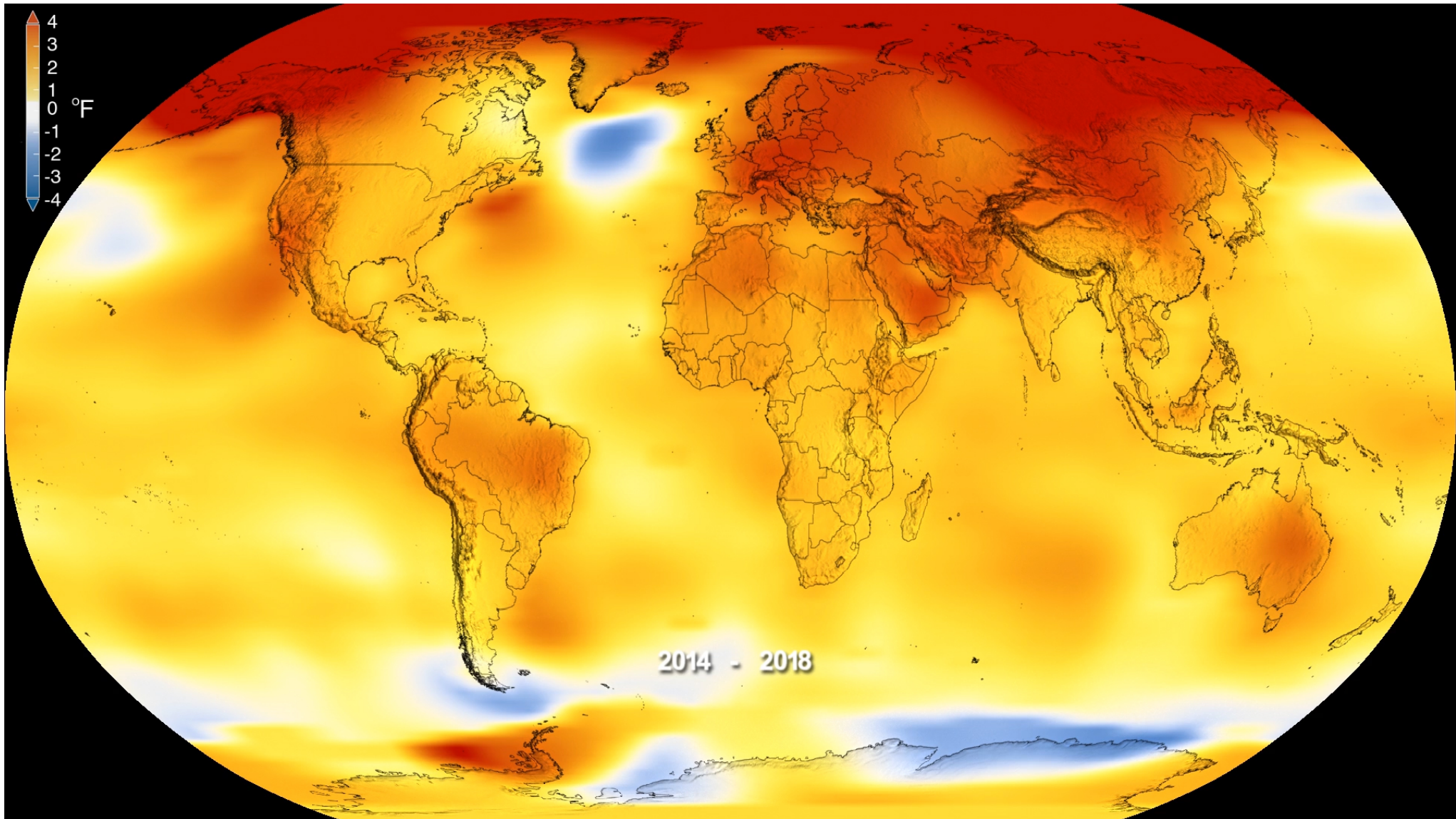
- Developed a new **numerical method** to solve the NS equations in **orthogonal** curvilinear coordinates (**FastRK3**)
- FastRK3 was verified and validated
 - Spatial convergence rate: **2nd order**
 - Temporal convergence rate: **3rd order**
- Developed **FFT-based Poisson solver** to solve pressure Poisson equation over orthogonal curvilinear grids \Rightarrow **FastPoc**
- FastPoc is **30-60 times faster** than Multigrid
- FastPoc takes **10%** of the CPU time of the NS solver FastRK3
- Applied to simulate the **flow over curved ramps and a bump**
- Next: Study turbulent (multiphase) flows w/o separation



Time:5



*Sit, be still, and listen, because you're drunk
and we're at the edge of the roof ~ Rumi*



<https://svs.gsfc.nasa.gov/13142>

Acknowledgments

- Parviz Moin for inviting me to CTR, Stanford Univ.
- Abhiram Aithal (Ph.D. student)
- Lt. Col. Barrett McCann (Ph.D. 2014) & Michael Dodd (Ph.D. 2017)
- Trefftz-Posada, Freund, Samuell (PhD students)
- Darren Adams (UIUC/NCSA)
- Said Elghobashi (UC, Irvine)
- JCATI/Boeing Co. Philippe Spalart
- NSF CAREER Award (2011)
- NSF XRAC Awards on XSEDE (2010-Present)
- IBM Bladecenter Hyak & HyakNG @ e-Science Institute (UW)
 - 34 nodes + 11 nodes dedicated to CFM research group
- Runs performed on XSEDE Comet (Dell w Intel Xeon E5)
 - FastRK3: 77% Navier-Stokes (RK3+post); 10% FastPoC-Poisson solver; 13% I/O
 - ~8 sec/time step on 256 cores for 1024x512x256 grid

